

1

2

3

Arbidol and other Low Molecular Weight Drugs That Inhibit Lassa and Ebola Viruses

4

5

6

7

Hulseberg CE^{a1}, Fénéant L^b, Szymańska-de Wijs KM^b, Kessler NP^b, Nelson EA^b,
Shoemaker CJ^{c2}, Schmaljohn CS^c, Polyak SJ^{d,e}, White JM^{a,b},

8

9

10

11

12

13

14

15

16

17

18

19

20

21

22

Abstract: 247 words

23

Importance: 147 words

24

Main Text: 5,187 words

25

26

27

28

Running Title: Drugs Targeting Ebola and Lassa Fever Virus Entry

29

30

31

32

33

Present addresses: Christine E. Hulseberg, Center for Genome Sciences, US Army Medical

34

Research Institute of Infectious Diseases, Fort Detrick, Maryland; C. Jason Shoemaker,

35

Diagnostic Systems Division, USAMRIID; Katarzyna Szymańska-de Wijs: Institute of Virology,

36

Hannover Medical School, 30625, Hannover, Germany

37

38

Corresponding author: Dept. of Cell Biology, Univ. of Virginia, 1340 Jefferson Park Ave.,

39

Charlottesville, VA, 22908-0732. Phone: (434) 924-2593. Fax: 434-982-3912. E-mail:

40

jw7g@virginia.edu

41

42 **Abstract**

43 Antiviral therapies that impede virus entry are attractive because they act on the first phase of the
44 infectious cycle. Drugs that target pathways common to multiple viruses are particularly
45 desirable when laboratory-based viral identification may be challenging, e.g. in an outbreak
46 setting. We are interested in identifying drugs that block both Ebola virus (EBOV) and Lassa
47 virus (LASV), two unrelated but highly pathogenic hemorrhagic fever viruses that have caused
48 outbreaks in similar regions in Africa and share features of virus entry: use of cell surface
49 attachment factors, macropinocytosis, endosomal receptors and low pH to trigger fusion in late
50 endosomes. Towards this goal, we directly compared the potency of eight drugs known to block
51 EBOV entry with their potency as inhibitors of LASV entry. Five drugs (amodiaquine, apilimod,
52 arbidol, niclosamide, and zoniporide) showed roughly equivalent inhibition of LASV and EBOV
53 glycoprotein (GP)-bearing pseudoviruses; three (clomiphene, sertraline and toremifene) were
54 more potent against EBOV. We then focused on arbidol, which is licensed abroad as an anti-
55 influenza drug and exhibits activity against a diverse array of clinically relevant viruses. We
56 found that arbidol inhibits infection by authentic LASV, inhibits LASV GP-mediated cell-cell
57 fusion and virus-cell fusion and, reminiscent of its activity on influenza hemagglutinin, stabilizes
58 LASV GP to low pH exposure. Our findings suggest that arbidol inhibits LASV fusion, which
59 may partly involve blocking conformational changes in LASV GP. We discuss our findings in
60 terms of the potential to develop a drug cocktail that could inhibit both LASV and EBOV.

61 **Importance**

62 Lassa and Ebola viruses continue to cause severe outbreaks in humans, yet there are only limited
63 therapeutic options to treat the deadly hemorrhagic fever diseases they cause. Because of
64 overlapping geographic occurrences and similarities in mode of entry into cells, we seek a

65 practical drug or drug cocktail that could be used to treat infections by both viruses. Towards this
66 goal, we directly compared eight drugs, approved or in clinical testing, for their ability to block
67 entry mediated by the glycoproteins of both viruses. We identified five drugs with approximately
68 equal potency against both. Among these we investigated the modes of action of arbidol, a drug
69 licensed abroad to treat influenza infections. We found, as shown for influenza, that arbidol
70 blocks fusion mediated by the Lassa virus glycoprotein. Our findings encourage the development
71 of a combination of approved drugs to treat both Lassa and Ebola virus diseases.

72

73 **Introduction**

74 Lassa virus (LASV) is an enveloped ambisense RNA virus belonging to the
75 Arenaviridae. As the most clinically significant member of this large family, LASV is a major
76 pathogen in West Africa, where it infects an estimated 300,000 people each year. LASV has also
77 been responsible for a number of imported cases of Lassa hemorrhagic fever (LHF) in Europe
78 and North America in recent years (1). The 2018 outbreak of LHF in Nigeria was particularly
79 severe, with over 430 confirmed positive cases and a case fatality rate of ~25% (2). Classic
80 symptoms of acute LHF include malaise, headache, fever, vomiting, respiratory distress, facial
81 edema, and hemorrhaging of mucosal surfaces (3). Even in fatal cases, however, patients may
82 not present with redolent hemorrhagic fever symptoms, complicating diagnosis (4).

83 The only antiviral treatment option for LHF is the guanosine analogue, ribavirin. There
84 are a substantial number of contraindications and adverse effects associated with ribavirin, and
85 its efficacy in clinical trial settings remains controversial and under-evaluated. Furthermore,
86 while ribavirin is effective against other hemorrhagic fever arenaviruses, it has limited efficacy
87 against filoviruses. Thus, current guidelines recommend ribavirin only after high-risk exposures

88 to LASV (5). Given the partial geographic overlap between EBOV and LASV in West Africa
89 and similar clinical presentation in early infection stages, it would be advantageous to have a
90 common therapeutic effective against both viruses (6, 7).

91 Promising new compounds against LASV have been identified (6, 8-17), but the limited
92 geographical endemicity of LASV, its inefficient person-to-person transmission, and low re-
93 infection rates make the prospect of collecting adequate clinical trial data on new drugs
94 challenging. Thus, a practical approach to more expeditiously grow the arsenal of drugs against
95 these highly pathogenic viruses is to screen approved drugs for antiviral activity. When this
96 strategy was employed, many FDA approved compounds with repurposing potential were
97 identified that showed inhibitory effects against EBOV (18-24). Many of these are thought to act
98 upon the entry stages of EBOV infection. A similar recent screen revealed FDA-approved drugs
99 with potential activity against LASV (8).

100 Viral entry inhibitors are valuable as therapeutics since blocking infection early in the
101 lifecycle will reduce cellular and tissue damage associated with the replication of incoming
102 viruses and the production of viral progeny. LASV employs several key features in common
103 with EBOV for its entry: 1) it is internalized into the endocytic pathway by a macropinocytotic-
104 like process after initial contact with surface receptors/attachment factors, 2) low pH is needed to
105 trigger fusion, and 3) an endosomal, cholesterol binding, receptor promotes endosomal escape
106 (Lamp1 for LASV and NPC1 for EBOV) (12, 25-32). Hence for this study, we selected eight
107 low molecular weight drugs shown to inhibit EBOV entry and directly compared their inhibitory
108 activity against LASV and EBOV. Five of these drugs have FDA approval (amodiaquine,
109 clomiphene, niclosamide, sertraline, and toremifene), one is licensed abroad (arbidol), and two
110 have been evaluated in clinical trials (apilimod and zoniporide).

111 The compound we investigated in most detail was the anti-influenza drug arbidol
112 (Umifenovir), which was developed and is currently used as an antiviral. Arbidol has been
113 reported to have inhibitory effects on a diverse array of viruses, including DNA and RNA viruses
114 as well as capsid- and membrane-enclosed viruses (33-36). Studies aimed at determining the
115 mechanism of action of arbidol implicate a number of possible antiviral effects, including several
116 steps of entry as well as later phases of the infectious cycle (36). The principle inhibitory effect
117 of arbidol on influenza virus, for which it has been a licensed treatment in China and Russia for
118 many years, appears to be during a late stage of entry, when influenza fuses with an endosomal
119 membrane. While arbidol can bind directly to influenza HA and inhibit its ability to transition to
120 an activated conformation (37-39), it is not yet clear whether this is its sole or primary
121 mechanism of anti-influenza activity, or if arbidol also impairs fusion by intercalation into the
122 viral or target membrane thereby rendering the membrane less yielding for fusion (35).

123

124 MATERIALS AND METHODS

125

126 **Chemicals and cell culture.** Dulbecco's modified Eagle's medium (DMEM), phenol-red free
127 DMEM, Opti-MEM (OMEM), sodium pyruvate, antibiotic/antimycotic, trypsin-EDTA 0.05%,
128 phenol-red free trypsin-EDTA 0.5 % and neutral red were from ThermoFisher Scientific.
129 Phosphate-buffered saline (PBS) was from Corning. Cosmic Calf Serum (CCS), Fetal Bovine
130 Serum (FBS) and Supplemented Calf Serum (SCS) were from HyClone. Fibronectin was from
131 Millipore. Polyethylenimine (PEI) and Non-Enzymatic Cell Dissociation Solution were from
132 Sigma. Lipofectamine 2000 was from Invitrogen. Toremfene citrate was from Selleck
133 Chemicals. Zoniporide, amodiaquine, niclosamide and clomiphene citrate were from Sigma.

134 Apilimod was from Axon MedChem. Sertraline HCl was from Toronto Research Chemicals.
135 Arbidol was synthesized commercially, and the purity and structure of the product were
136 confirmed as described previously (34).

137 HEK293T/17 and BSC-1 cells were from the ATCC, Lamp1 KO HEK293T/17 cells
138 (clone 1D4) were described in Hulseberg et al., 2018. COS7 cells were from the ATCC and a
139 kind gift from Douglas DeSimone at the University of Virginia. BHK-21 cells were from the
140 ATCC and a kind gift from James Casanova at the University of Virginia. Vero76 cells were
141 from the United States Army Medical Research Institute of Infectious Diseases (USAMRIID).
142 HEK293T/17 and BSC-1 cells were maintained in DMEM containing 10% CCS. BHK21 cells
143 were maintained in DMEM containing 10% SCS. COS7 and Lamp1 KO HEK293T/17 cells were
144 maintained in DMEM containing 10% FBS, 1% sodium pyruvate, and 1% antibiotic/antimycotic.
145 Vero76 cells were maintained in Corning DMEM with 10% Gibco FBS, 1%
146 penicillin/streptomycin, 1% L-Glutamine, and 1% sodium-pyruvate.

147

148 **Plasmids and Virus.** The pCMV-LASV-GPC Josiah strain plasmid was from F.L. Cosset
149 (Université de Lyon, France) via Gregory Melikian (Emory University), the LASV-GPC-Flag
150 pCC421 Josiah strain was from Jason Botten (University of Vermont). VSV-G plasmid was from
151 Michael Whitt (University of Tennessee); pDisplay-EBOV-GPΔ Mayinga strain was from Erica
152 Sapphire (Scripps Research Institute). TG-Luc plasmid was from Jean Dubuisson (Centre
153 National de la Recherche Scientifique, Lille, France) via Gary Whittaker (Cornell University),
154 pCMV-Gag-Pol plasmid was from Jean Millet and Gary Whittaker (Cornell University) and Jean
155 Dubuisson; Gag-βlaM plasmid was made by James Simmons (University of Virginia). The
156 pcDNA3-luciferase (Firefly) plasmid was from Addgene. The DSP₁₋₇ and DSP₈₋₁₁ plasmids were

157 from Naoyuki Kondo (Kansai Medical University, Japan). The WSN HA and NA plasmids were
158 from Gary Whittaker (Cornell University). Plasmids encoding LCMV GP and Junin GP were
159 from Jack Nunberg (University Montana).

160 The stock of LASV (Josiah strain) used was generated by infecting Vero E6 cells in
161 complete EMEM (VWR) containing 10% FBS (HyClone) and 2% L-Glutamine (ThermoFisher
162 Scientific). Infected cells were incubated at 37°C/5% CO₂. Virus-containing cell culture
163 supernatant was harvested 3 days post-inoculation, clarified at 10,000 x g at 4°C for 10 min, and
164 frozen at -80°C. All work with native LASV was conducted in a BSL4 containment suite with
165 personnel in positive pressure encapsulating suits following appropriate institutional SOPs.

166

167 **Antibodies and immunoprecipitation reagents.** For western blotting, the mouse-anti-LASV-
168 GP L52-134-23A was from USAMRIID and anti-mouse-IR680RD was from Licor. For LASV
169 GP bead capture, α -Flag@M2 magnetic beads were from Sigma.

170

171 **Pseudovirus production.** To produce VSV pseudoviruses, 1 x 10⁶ BHK-21 cells were seeded in
172 each of multiple 10 cm² dishes. Cells in each dish were transfected with 12 μ g of plasmid
173 encoding LASV-GPC using PEI. The following day, cells were infected with 40 μ l (per dish)
174 VSV- Δ G helper virus (from pre-titered plaque eluate) encoding *Renilla* luciferase (diluted in
175 serum-free media) for 1 hr at 37°C. After infection, cells were washed extensively with cold PBS
176 and incubated overnight in complete DMEM. Supernatants containing pseudoviruses were
177 collected, clarified and pelleted through a 20% sucrose-HM (20 mM HEPES, 20 mM MES, 130
178 mM NaCl, pH 7.4) cushion. The pellet was re-suspended in 10% sucrose-HM. VSV- Δ G helper

179 virus was produced following the same procedure, by infecting VSV-G transfected cells with
180 eluate from VSV-ΔG plaques.

181 For MLV pseudoviruses, HEK293T/17 cells were seeded in 10 cm² dishes. The following
182 day, cells were transfected with 6 μg of total DNA using a 2:1:1:1 ratio of pTG-Luc:pCMV Gag-
183 Pol:Gag-βlam:glycoprotein. At 48 hr post-transfection, virus-containing medium was harvested,
184 clarified, pelleted through a 20% sucrose-HM cushion, resuspended in 10% sucrose-HM, and
185 stored at -80°C in single use aliquots.

186

187 **LASV plaque reduction assay.** Vero76 cells were seeded on 6-well plates. At full confluency,
188 cells in duplicate wells were pretreated with the indicated concentration of arbidol, 25 mM
189 NH₄Cl, or 10% ethanol vehicle for 1 hr at 37°C. Cells were then infected with LASV at a
190 multiplicity of infection (MOI) of 0.01 for 1 hr in the presence of the indicated concentration of
191 arbidol or vehicle. Cells were washed twice to remove unbound virus and incubated for 24 hr at
192 37°C in drug-containing medium. Supernatants were harvested and 10-fold serial dilutions were
193 made to infect ~90% confluent monolayers of Vero76 cells in 6-well plates for 1 hr at 37°C, with
194 rocking every 15 min. A primary overlay consisting of a 1:1 mixture of 1.6% SeaKem agarose
195 (Lonza) and 2x EBME (ThermoFisher Scientific) supplemented with 20% FBS and 8%
196 Glutamax (ThermoFisher Scientific) was then added on top of the infected cells and allowed to
197 solidify. Cells were incubated for 4 days at 37°C, followed by addition of a secondary overlay
198 consisting of a 1:1 mixture identical to the above but with the addition of 8% Neutral Red (final
199 NR concentration was 4%). Plaques were counted the following day. Plaque counts were
200 averaged from duplicate wells and then multiplied by dilution factor to establish starting titer of
201 input supernatants.

202

203 **Biosafety.** All manipulations involving live LASV were performed in a biosafety level 4
204 containment suite at USAMRIID with personnel wearing positive-pressure protective suits fitted
205 with HEPA filters and umbilical fed air. USAMRIID is registered with the Centers for Disease
206 Control Select Agent Program for the possession and use of biological select agents and toxins
207 and has implemented a biological surety program in accordance with U.S. Army regulation AR
208 50-1 “Biological Surety.”

209

210 **Pseudovirus Infection assay.** BSC-1 cells were seeded on white 96-well plates (1.5×10^4
211 cells/well). The following day, cells were pretreated with drugs (or mock) for 1 hr in OMEM and
212 then, while maintaining the presence of drug, were infected with an input of EBOV GP- and
213 LASV GP-pseudoviruses that had been pre-titered to achieve roughly equivalent RLU signals in
214 the mock-treated samples. After 24 hr at 37°C/5% CO₂, the cells were lysed with Britelite
215 reagent (PerkinElmer) and luminescence was measured. IC₅₀ concentrations and statistical
216 analysis of all data were performed using GraphPad Prism 7 (GraphPad Software, Inc.):
217 Log(Agonist) vs. response-variable slope (four parameters) constrained to bottom=0.

218

219 **Cell-cell fusion (CCF) assay.** Effector (HEK293T/17) cells were seeded on 6-well plates ($6.75 \times$
220 10^5 cells/well). Target (HEK293T/17) cells were seeded on fibronectin-coated opaque white 96-
221 well plates (3.5×10^4 cells/well). Effector cells were transfected with 1 µg/well of GP plasmid
222 and 1 µg/well of DSP₁₋₇ plasmid. Target cells were co-transfected with 33 ng/well pmLamp1 and
223 33 ng/well of DSP₈₋₁₁ plasmid. Cells were transfected using Lipofectamine 2000, according to
224 the manufacturer’s instructions. Twenty-four hours post-transfections, effector cells were loaded

225 with EnduRen™ luciferase substrate (Promega) (60 μ M in complete DMEM) for 2 hr at 37°C.
226 Effector cells were then rinsed with PBS and lifted with Non-Enzymatic Cell-Dissociation
227 Solution. Effector cells were re-suspended in complete DMEM and 1×10^5 effector cells were
228 overlaid onto each well of target cells (96-well plate). Cells were co-cultured for 3 hr. At this
229 time, a low pH pulse was applied with fusion buffer (100mM NaCl, 15 mM HEPES, 15 mM
230 succinate, 15 mM MES, 2 mg/mL glucose) adjusted to pH 5.0, for 5 min at 37°C. The pH was re-
231 neutralized by replacing the fusion buffer with complete DMEM, and the cells were returned to
232 37°C for 1 hr before measuring luciferase activity.

233

234 **Forced fusion at the plasma membrane (FFPM) assay.** COS7 cells were seeded in 6-well
235 plates (4×10^5 cells/well). ~24 hr post seeding, the cells were transfected with 1 μ g of plasmid
236 encoding firefly luciferase using Lipofectamine 2000 according to the manufacturer's
237 instructions. ~24 hr post transfection, the cells were washed, lifted, and reseeded at 1.5×10^4
238 cells/well on fibronectin-coated opaque white 96-well plates. The day after re-seeding, cells were
239 chilled on ice for 15 min and LASV-GP VSV-luciferase (*Renilla*) pseudoviruses, which had been
240 titered to reach a target signal of at least 1×10^6 RLU in a standard infection assay, were added
241 to cells in quintuplicate in serum-free DMEM. Pseudoviruses were bound to the cells by
242 centrifugation (250 x g, 1 hr, 4°C). Cells were returned to ice and washed once with cold PBS.
243 Fusion was triggered by applying a pulse of pre-warmed low pH fusion buffer (as in CCF assay)
244 for 5 min at 37°C adjusted to the indicated pH values. Cells were returned to ice and the fusion
245 buffer was replaced with complete DMEM containing 40 mM NH_4Cl (to block virus entry via
246 the normal endocytic route) was added. Sixteen hr later, luciferase activity was measured using
247 the Dual-Glo® Luciferase Assay System (Promega) according to the manufacturer's instructions

248 using a Promega GloMax® luminometer. The ratio of *Renilla* luciferase activity (an indicator for
249 pseudovirus infection) over firefly luciferase activity (to account for the number of cells) was
250 calculated to assess viral GP-mediated fusion with the plasma membrane.

251

252 **GP1 dissociation assay.** Lamp1 KO HEK293T/17 cells were seeded in 6-well plates (6.25×10^5
253 cells/well). The following day, cells were transfected with 1 μg of LASV-GPC-Flag using PEI.
254 At 48 hr post-transfection, the cells were lysed with NETI buffer (150 mM NaCl, 1 mM EDTA,
255 50 mM Tris-HCl, 0.5% Igepal) at pH 8. After clearing cell debris (centrifugation for 15 min at
256 21,000 x g), the lysate was incubated with α -Flag® M2 Magnetic Beads (that were prewashed
257 twice in NETI buffer pH 8) for 1 hr at 4°C. Arbidol was then added to the bead plus lysate
258 mixture as indicated, and the samples were incubated for an additional hour at 4°C. For pH-
259 dependent dissociation experiments, beads with captured LASV GP and pretreated +/- arbidol
260 were then pulled over on a magnetic stand and quickly washed with cold NETI buffer (without
261 arbidol) at the indicated pH. The cold NETI buffer was then replaced with pre-warmed NETI
262 buffer at the same pH +/- arbidol, as indicated. Samples were incubated at 37°C for 1 min. For
263 time-dependent dissociation experiments, beads with captured LASV GP and pretreated +/-
264 arbidol as above were quickly washed with cold NETI buffer at pH 6.5. The cold pH 6.5 buffer
265 was then replaced with pre-warmed NETI buffer at pH 6.5 +/- arbidol. Samples were then
266 incubated at 37°C for 0.5, 1.0, 2.5 or 5.0 min. The “0 min” samples were treated with pre-
267 warmed buffer, and then placed immediately on ice post buffer addition. At the end of the
268 indicated incubation period, the samples were immediately placed on the magnetic rack and
269 supernatants collected. Proteins were then eluted from the residual beads using 100 mM glycine
270 pH 3.5 for 15 min at 25°C with constant vortexing, and the eluted samples were neutralized by

271 the addition of 1M Tris-HCl, pH 8.5. Supernatant and bead samples were then analyzed by SDS-
272 PAGE and western blotting, with a primary antibody against LASV GP1. The signal intensity of
273 the GP1 bands in the supernatant and corresponding bead samples was measured using ImageJ.
274 Percent GP1 dissociation was calculated as the signal intensity of the GP1 band in the
275 supernatant divided by the summed signal intensity of the GP1 bands in the supernatant and bead
276 samples.

277

278

279 **RESULTS**

280

281 **Comparison of the potency of small molecule inhibitors against LASV GP- and EBOV GP-**
282 **mediated entry.** Enveloped viruses that are endocytosed rely on their glycoproteins (GPs) to
283 mediate the entire entry process, from attachment to the cell surface to fusion within endosomal
284 membranes. Here we directly compared the effects of eight drugs that block EBOV entry for
285 their effects on LASV GP-mediated entry. To do this, we used murine leukemia viruses (MLV)
286 carrying a luciferase reporter and pseudotyped with either LASV or EBOV GP. Drug dosing
287 ranges were determined by establishing the concentration of each drug needed to elicit a near-
288 total inhibition of infection. The remaining doses in each set were 2-fold serial dilutions. A mock
289 (vehicle-only) treatment was included as an anchor point in each series to assess the extent of
290 inhibition in treated cells.

291 Representative direct comparative dose response curves for LASV and EBOV for each of
292 the eight drugs are presented in Fig. 1. Each drug was tested in parallel against LASV GP- and
293 EBOV GP-MLV pseudoviruses in three to five independent experiments. Table 1 reports the

294 average ratio of the IC_{50} value against LASV GP divided by that for EBOV GP, analyzed in
295 parallel, for each of the eight drugs tested. These ratios indicated that the IC_{50} values against
296 LASV GP-MLV pseudoviruses for five drugs (zoniporide, amodiaquine, niclosamide, apilimod,
297 and arbidol) were either approximately the same or lower than the corresponding values for
298 EBOV GP-MLV pseudoviruses, indicating similar or enhanced potency against LASV GP-
299 mediated infection. For three drugs, clomiphene, sertraline and toremifene, the IC_{50} values for
300 LASV are ~3-6-fold greater than those for EBOV, indicating that these drugs are more potent
301 against EBOV. It is noteworthy that the latter three drugs are cationic amphiphilic drugs (CADs),
302 which may be especially active against EBOV (19, 20, 23, 40).

303 For the remainder of the study we focused on arbidol, for reasons outlined in the
304 introduction. Pécheur and colleagues reported an EC_{50} of 5.8 μ M in Vero cells for arbidol against
305 the New World arenavirus, Tacaribe virus; to the best of our knowledge the latter is the only
306 published evaluation of the efficacy of arbidol against an arenavirus. Using MLV pseudoviruses
307 we found that in addition to inhibiting entry mediated by LASV GP (Fig. 1), arbidol inhibited
308 entry mediated by the GPs of two other arenaviruses, those of LCMV and Junin (Fig. 2A). We
309 also found, using MLV pseudoviruses, that arbidol is somewhat more potent against LASV GP-
310 mediated infection than against infection mediated by influenza HA from the WSN (H1N1)
311 strain (Fig. 2B).

312

313 **Arbidol blocks authentic LASV infection.** To evaluate the efficacy of arbidol against authentic
314 LASV, we performed LASV (Josiah) plaque reduction assays under BSL4 conditions, testing the
315 effects of concentrations of arbidol up to 40 μ M. Cells were pretreated with arbidol for 1 hr and
316 then infected with LASV (Josiah) in the continued presence of arbidol for 24 hr. In the first of

317 three experiments the IC_{50} was ~ 5 - $10 \mu\text{M}$ and the maximum inhibition was 98% (Fig. 3A); in
318 the second, the IC_{50} was $\sim 20 \mu\text{M}$ and the maximum inhibition was 100% (Fig. 3B). In a third
319 experiment, testing only $20 \mu\text{M}$ arbidol, the percent inhibition was 74% (Fig. 3C). The average
320 percent inhibition caused by $20 \mu\text{M}$ arbidol from the three experiments was 72.5% (Fig. 3D). By
321 visual inspection $40 \mu\text{M}$ arbidol had no effect on Vero cell monolayers for up to five days (data
322 not shown). We note that the apparent IC_{50} for arbidol vs. authentic LASV (Fig. 3) is higher than
323 that seen with MLV pseudoviruses bearing LASV GP (Figs. 1 and 2).

324

325 **Arbidol blocks LASV GP-mediated fusion.** We next asked if arbidol impairs LASV GP-
326 mediated fusion, as it does for other viruses (33, 35, 38, 39, 41). Given that optimal LASV fusion
327 requires the endosomal protein Lamp1 (26, 31, 42), we used cells expressing Lamp1 at the
328 plasma membrane (pmLamp) as fusion targets. Cell-cell fusion (CCF) was then induced between
329 co-cultured effector cells (expressing LASV GP at their surface) and target cells (expressing
330 Lamp1 at their surface) by briefly exposing the cells to low pH, as described previously (31). To
331 assess the effects of arbidol, effector cells (expressing LASV GP) were pretreated for 1 hr with
332 the indicated concentration of arbidol, co-cultured with pmLamp1-expressing target cells, and
333 then triggered to fuse by brief exposure to pH 5 (all in the continued presence of arbidol). The
334 efficiency of CCF was then determined by measuring the activity of the luciferase reporter that is
335 functionally restored upon cytoplasmic mixing of fused cells (43). As seen in Fig. 4A, CCF by
336 LASV GP (at pH 5.0) was suppressed by $20 \mu\text{M}$ and $40 \mu\text{M}$ arbidol. Based on findings in
337 parallel experiments (Fig. 4B), arbidol appeared more potent at impeding LASV-GP than
338 influenza HA-mediated CCF, consistent with its somewhat stronger effect on LASV GP-
339 compared to influenza HA-MLV pseudovirus infection (Fig. 2B).

340 As a complement to the CCF study (Fig. 4), we employed a forced fusion at the plasma
341 membrane (FFPM) assay and assessed fusion of LASV GP-VSV pseudoviruses with the surface
342 of cells expressing pmLamp1 (i.e., with Lamp1 at the cell surface), as previously described (31).
343 As seen in Fig. 5A, arbidol suppressed LASV-GP-mediated FFPM with strong and complete
344 inhibition seen with 20 and 40 μ M doses, respectively. The experiment shown in Fig. 4A was
345 conducted with a low pH pulse of pH 5.0. As seen in Fig. 5B, 40 μ M arbidol strongly inhibited
346 LASV GP-mediated FFPM at both pH 5.0 and pH 5.5.

347

348 **Effects of arbidol on LASV GP1 dissociation.** In the case of influenza, arbidol stabilizes HA
349 (the fusion protein) such that the pH dependence for its fusion-inducing conformation change is
350 shifted by 0.2-0.3 units in the more acidic direction (37, 39). Stabilization of HA is considered
351 part of the mechanism of arbidol against influenza virus (38, 39, 44, 45). Since two independent
352 assays (CCF and FFPM) showed that arbidol impairs the fusion activity of LASV GP, we next
353 asked whether it impairs a conformational change in GP1 required for fusion activation. Upon
354 exposure to low pH, LASV GP undergoes structural rearrangements, one of the earliest being
355 dissociation of GP1, the receptor binding subunit, from GP2, the fusion subunit. This early
356 change is thought to license subsequent changes that allow the fusion loop (in GP2) to access the
357 target membrane and then to permit GP2 to fold back into a trimer-of-hairpins, which brings the
358 viral and endosomal membranes into intimate contact leading to their fusion (46-49).
359 Experiments using isolated LASV GP1/GP2 captured on beads showed that in this system,
360 dissociation of the 44 kDa GP1 subunit occurs optimally at 37°C and half maximally at pH ~6.4
361 at 37°C following a 1 min low pH pulse (data not shown). We therefore treated LASV GP1/GP2
362 immobilized on beads with either 0 or 40 μ M arbidol and then exposed the beads to buffers of

363 different pH values for 1 min at 37°C. As seen in Fig. 6A, the presence of 40 μM arbidol shifted
364 the pH dependence for GP1 dissociation by ~0.5 units in the more acidic direction, suggesting
365 that, as for influenza HA, arbidol can stabilize LASV GP. If arbidol stabilizes LASV GP, then it
366 might delay GP1 dissociation in this system. To test this idea, we again captured LASV
367 GP1/GP2 on beads, pre-treated the samples with 0 or 40 μM arbidol, treated the beads at pH 6.5
368 and 37°C in the presence of arbidol, and then took samples from 0-5 min and assayed them for
369 GP1 dissociation. As seen in Fig. 6B, arbidol appeared to introduce an ~30 second lag, thereby
370 slowing GP1 dissociation.

371

372 DISCUSSION

373 **Drugs that block LASV- and EBOV GP-mediated entry with similar potency.** We began this
374 study by comparing the ability of eight drugs to inhibit LASV and EBOV GP-mediated
375 infection. All eight are orally available, room temperature stable small molecules that block
376 EBOV entry (18-20, 22, 23, 40, 50) and target entry processes also used by LASV (20-23, 51-
377 53). Six are approved for clinical use and two are in advanced clinical testing. These collective
378 features offer practical advantages (e.g., net costs and ease of transport and delivery) compared
379 to novel drugs, many of which are designed in a ‘one drug-one bug’ approach (54).

380 Five drugs showed similar potency against LASV- and EBOV GP-mediated entry (Table
381 1). Zoniporide, an inhibitor of the plasma membrane Na⁺/H⁺ exchanger, blocks infection by the
382 arenavirus LCMV by thwarting macropinocytotic uptake of viral particles (52). As both LASV
383 (30) and EBOV (55, 56) are taken into cells by macropinocytosis, we expected and found
384 zoniporide to have similar activity against both. Two drugs that impair endosome acidification,
385 needed for the entry of both viruses (25, 49)---amodiaquine (an antimalarial) and niclosamide (an

386 anthelmintic)---also showed similar potency against both viral GPs in our direct comparative
387 tests. Both have been shown, albeit not in direct comparative studies, to inhibit many pathogens
388 that enter cells by endocytosis (21-23, 57-60). The fourth drug with similar activity against both
389 viruses is apilimod, which inhibits PIKfyve, an enzyme required for late endosome maturation
390 (51, 53, 61) and EBOV entry (27). Apilimod blocks EBOV trafficking to late endosomes (51,
391 53), which serve as portals for both EBOV and LASV (25, 26, 62-64). The fifth drug with
392 similar potency against LASV GP- and EBOV GP- mediated entry is arbidol (Umifenovir), a
393 synthetic antiviral approved and used in Russia and China to combat influenza, and shown to
394 have broad-spectrum antiviral activity (33, 34, 36, 38, 39).

395 The other three drugs---clomiphene, toremifene, and sertraline---showed ~3-6-fold
396 greater activity against EBOV GP than LASV GP-mediated entry. They are CADs that block
397 EBOV infections (19, 20, 22, 23, 40) and cause cholesterol accumulation in late endosomes,
398 mimicking effects of dysfunctional NPC1, the EBOV receptor (27, 28, 65). Since LASV also
399 enters cells through late endosomes (31), CADs may interfere with LASV entry due to general
400 impairments of late endosome function. The enhanced activity of toremifene and sertraline
401 against EBOV (Table 1), may be because they can bind to both EBOV GP, as shown by thermal
402 stability assays and X-ray crystallography (66, 67), as well as to the viral and/or endosomal
403 membrane (35, 39, 45, 66).

404

405 **Mechanisms by which arbidol may block LASV entry and infection.** Arbidol showed
406 roughly equivalent potency against LASV and EBOV GP-mediated pseudovirus infection (Fig.
407 1, Table 1), blocked infection by authentic LASV (Fig. 3), and was somewhat more effective at
408 blocking LASV GP- vs. influenza HA-mediated fusion and entry (Figs. 2B and 4B). Three

409 mechanisms have been proposed for the action of arbidol against influenza: direct binding to HA
410 (K_d 47 μ M to PR8 influenza HA) (38, 44) and, as proposed for other viruses, binding to the viral
411 and/or target membrane so as to reduce fusion fitness (34, 35). By binding to and stabilizing
412 HA, arbidol shifts the pH threshold for fusion-inducing conformational changes by \sim 0.2 to 0.3
413 units in the more acidic direction (37, 38). This is noteworthy as even such small changes in
414 fusion pH can significantly impact influenza infectivity (67). Similarly, we found that arbidol
415 shifts the pH dependence for LASV GP1 dissociation from GP2 by \sim 0.5 units (in the more acidic
416 direction). This event is thought to unclamp the LASV fusion subunit (GP2), analogous to the
417 unclamping of influenza HA2 and HIV gp41. Hence, in addition to its likely general fusion-
418 impairing effects caused by intercalation into the viral and/or endosomal membrane (35, 45, 66),
419 it is plausible that arbidol additionally affects the stability of LASV GP in a manner similar to its
420 effects on influenza HA (37-39). And, as reviewed elsewhere (36), arbidol may also affect steps
421 upstream or downstream of fusion.

422

423 **Therapeutic potential of drugs with similar potency against LASV and EBOV.** As reasoned
424 in the Introduction, a long-term goal is to identify a drug cocktail that inhibits both LASV and
425 EBOV. Our focus is on orally available, room temperature stable drugs that target processes used
426 in common for LASV and EBOV entry into cells. Here we identified five drugs that target
427 discrete steps of entry and show approximately equal potency against LASV and EBOV GP-
428 mediated entry: the macropinocytosis inhibitor, zoniporide; the endosome acidification inhibitors
429 amodiaquine and niclosamide; the trafficking inhibitor, apilimod; and the fusion inhibitor,
430 arbidol.

431 While zonisamide is not approved, it has advanced to Phase II clinical trials for treatment
432 of cardiovascular diseases. As an alternate, the FDA-approved drug aripiprazole (trade name
433 Abilify) may have utility. Aripiprazole blocks EBOV infection and synergizes with other entry
434 inhibitors (20, 23). Preliminary data suggest that it blocks EBOV particle internalization as well
435 as LASV GP-mediated infection (White Lab, unpublished data). The endosome acidification
436 inhibitors amodiaquine and niclosamide are orally available and FDA-approved to treat malaria
437 and helminthic diseases, respectively. For both, the C_{max} is within range of the IC_{50} for anti-
438 EBOV/LASV activity (20-23, 57, 68, 69). Newer amodiaquine derivatives (59) or synergistic
439 drug pairs containing amodiaquine or niclosamide and another agent could lower the needed
440 doses (23). And while the trafficking inhibitor apilimod is well tolerated and a potent antagonist
441 of EBOV and LASV (51, 53, 70) (and this study), in a first test, it did not protect mice from
442 lethal EBOV challenge (see (23)), likely due to its inhibition of IL12/23 production ((61) and
443 Rogers et al, manuscript submitted).

444 Among the fusion inhibitors tested, arbidol emerges as a candidate for future
445 consideration, as it shows similar activity against LASV and EBOV and appears, in our assays,
446 somewhat more potent against LASV- and EBOV GP- vs. influenza HA-mediated fusion and
447 entry. Arbidol is approved and used in China and Russia against influenza and has shown
448 strikingly broad anti-viral activity (33, 36, 71). A single standard human dose (200 mg) of
449 arbidol yields a C_{max} lower (33, 72-74) than our preliminary indication (Fig. 3) of its IC_{50} against
450 authentic LASV. We note, however, that the estimated IC_{50} s for arbidol against authentic LASV
451 (Fig. 3) and influenza (39, 45, 75) are similar (roughly $\sim 10 \mu M$; variable for different influenza
452 strains). As standard dosing of arbidol for influenza is 200 mgs three (72) or four (75) times per
453 day, and as arbidol has a long half-life (36), the net (cumulative) C_{max} with multiple daily dosing

454 is expected to be significantly higher (S. Polyak and M. Paine, unpublished calculation). Hence,
455 as standard dosing of arbidol is clinically beneficial against influenza (see for example, (75)), it
456 may have utility against LASV and EBOV. However, the only modest reduction in titer seen
457 (Fig. 3) coupled with experience with another hemorrhagic fever virus (76) argue against
458 proposing arbidol as a stand-alone therapeutic. A tolerated higher dose of arbidol (74), a new
459 arbidol derivative (39, 44), or a combination of arbidol with another drug (23, 77, 78) might
460 lower the dose needed to be in line with attainable anti-viral efficacy. With respect to a potential
461 drug cocktail including arbidol, it is interesting that amantadine, rimantadine, ribavirin, and
462 ribamidil have been reported to enhance the activity of arbidol against influenza (79).

463 We envision that an orally-available, room temperature stable, approved drug or cocktail
464 of approved drugs could be rapidly deployed for treatment or prophylaxis against (suspected)
465 cases of LASV and EBOV, especially in regions around the globe that are challenged in terms of
466 resources, infrastructure and accessibility. Such a drug, or drug cocktail, might be valuable
467 before a definitive diagnosis has been made, concurrent with vaccination (e.g., of healthcare
468 workers and/or first responders to outbreaks), and/or during the set-up of ring vaccination. Here
469 we have identified several drugs with these attributes that show similar inhibition of LASV and
470 EBOV entry. Moreover, three of them---amodiaquine, niclosamide, and arbidol---inhibit
471 multiple enveloped viruses (33, 36, 57, 60, 71, 80-83). Hence, a drug or drug cocktail containing
472 these drugs could inhibit multiple enveloped viruses that enter cells through the endocytic
473 pathway (49).

474

475 **ACKNOWLEDGEMENTS**

476 The authors thank Dr. Aura Garrison (USAMRIID) for her generous gift of the LASV virus
477 stock used in the plaque reduction assays. We also thank Mary Paine, Washington State

478 University, for helpful discussions on how to calculate drug accumulation indices. The work was
479 supported by NIH RO1 AI114776 (to JMW).
480

481
482
483

Drug	Step Blocked	n	Average Ratio (+/- SEM) IC ₅₀ LASV/ IC ₅₀ EBOV
Zoniporide	Internalization	3	0.72 +/- 0.14
Amodiaquine	Acidification	4	0.41 +/- 0.14
Niclosamide	Acidification	5	0.54 +/- 0.13
Apilimod	Traffic	3	1.50 +/- 0.16
Arbidol	Fusion	3	0.59 +/- 0.12
Clomiphene	Fusion	4	4.72 +/- 2.41
Sertraline	Fusion	3	4.99 +/- 2.37
Toremifene	Fusion	3	6.71 +/- 3.09

484
485
486
487
488
489
490
491
492
493
494
495
496
497
498
499
500

Table 1: Comparative ability of drugs to block infections by LASV- and EBOV GP-MLV pseudoviruses. In each experiment (n=3-5 as indicated) cells were pretreated with 8 doses of the indicated drugs and their IC₅₀s for blocking infections by LASV and EBOV GP MLV pseudoviruses were determined in triplicate samples as described in the Materials and Methods section. For each experiment, the following ratio was then calculated: the IC₅₀ for blocking LASV GP pseudovirus infection divided by the IC₅₀ for blocking EBOV GP pseudovirus infection. Values in column 4 are the averages of those ratios +/- SEM. The average IC₅₀ and maximal percent inhibition values across all experiments for LASV were: zoniporide (88 μM, 87%), amodiaquine (1.9 μM, 82%), niclosamide (0.12 μM, 100%), apilimod (0.04 μM, 80%), arbidol (1.7 μM, 95%), clomiphene (5.7 μM, 100%), sertraline (2.6 μM, 90%), toremifene (2.9 μM, 96%). The average IC₅₀ and maximal percent inhibition values across all experiments for EBOV were: zoniporide (115 μM, 98%), amodiaquine (6.6 μM, 97%), niclosamide (0.24 μM, 100%), apilimod (0.03 μM, 100%), arbidol (2.8 μM, 100%), clomiphene (1.8 μM, 100%), sertraline (0.7 μM, 100%), toremifene (0.5 μM, 100%). Very similar ratios to those presented in column 4 above were obtained for the ratios of the average IC₅₀ values across all experiments.

501

502 **FIGURE LEGENDS**

503

504 **FIG 1. Representative dose response curves for eight low molecular weight drugs against**
505 **LASV GP- and EBOV GP-mediated MLV pseudovirus infection.** BSC-1 cells were
506 pretreated with the indicated dose of the indicated drug for 1 hr and then infected with MLV
507 pseudoviruses encoding luciferase. Luciferase signals were measured 24 hr later and normalized
508 to the maximal signal from a triplicate set of mock-treated cells. Data points indicate the average
509 % inhibition from triplicate wells. Error bars represent the standard deviation (SD). The red
510 horizontal dashed line indicates 50% inhibition. Each dose response comparison was conducted
511 3-5 times, with similar results.

512

513 **FIG 2. Comparative effects of arbidol on infection by MLV pseudoviruses bearing LASV**
514 **or other viral glycoproteins: (A) LASV, LCMV, and Junin GP; (B) LASV GP and**
515 **influenza HA.** MLV pseudoviruses bearing LASV GP, LCMV GP, Junin GP, or WSN influenza
516 HA and NA were prepared as described in the Materials and Methods section. BSC-1 cells were
517 pre-treated with the indicated concentrations of arbidol and then processed and analyzed for
518 infection as described in the legend to Fig. 1. Data in (A) are the averages +/- SEM from three
519 experiments, each performed with triplicate samples. Data in (B) represent the average +/- SD
520 from triplicate samples from one experiment.

521

522

523 **FIG 3. Arbidol inhibits authentic LASV infection.** Duplicate wells of Vero76 cells were
524 pretreated with the indicated concentration of arbidol (or vehicle or 25 mM NH₄Cl) for 1 hr and
525 then infected with LASV (Josiah strain) virus at an MOI of 0.01. Following a 1 hr binding period
526 at 4°C, unadsorbed virus was removed and the cells were incubated for 24 hr in the presence of
527 drug in a 37°C CO₂ incubator. Culture supernatants were harvested, serially diluted 10-fold in
528 fresh medium, and then titered on Vero76 cells by a 96 hr plaque assay. Results in (A-C) are the
529 average titers from duplicate wells. The values in (D) indicate the average normalized infection
530 in samples treated with 20 μM arbidol (+/- SD) from the experiments shown in (A-C). The
531 asterisk indicates **p < 0.01.

532

533 **FIG 4. Arbidol suppresses LASV GP-mediated cell-cell fusion (CCF).** Effector cells were
534 generated by transfecting HEK293T/17 cells with plasmids encoding DSP₁₋₇ (the N-terminal
535 split luciferase plasmid) and either (A) LASV GP or (B) WSN influenza HA and NA. Target
536 cells were generated by transfecting HEK293T/17 cells with plasmids encoding DSP₈₋₁₁ (the C-
537 terminal split luciferase plasmid) and pmLamp1. For the experiments, effector cells were
538 preloaded with a luciferase substrate and then pretreated for 1 hr with the indicated concentration
539 of arbidol or 10% EtOH (mock control). Effector cells were then co-cultured with target
540 HEK293T/17 cells (in the continued presence of arbidol or 10% EtOH) for 3 hr at 37°C. At this
541 time the cultures were pulsed with pH 5 buffer for 5 min at 37°C, reneutralized and then returned
542 to the 37°C CO₂ incubator for 1 hr, at which time the luminescent signal was measured. The data
543 represent the normalized luminescent signal (relative to mock-treated controls) from three
544 experiments, each performed with triplicate samples. Error bars indicate SD. Asterisks indicate:
545 *p < 0.05, **p < 0.01, and ***p < 0.001.

546

547 **FIG 5: Arbidol inhibits LASV-GP-mediated forced fusion at the plasma membrane**
548 **(FFPM).** COS7 cells were transfected with plasmids encoding pmLamp1 and firefly luciferase
549 (FLUC). Roughly 24 hr later, the cells were pretreated with the indicated dose of arbidol (or
550 mock treated) for 1 hr. At this time, VSV pseudoviruses bearing LASV GP and encoding *Renilla*
551 luciferase (RLUC) were allowed to bind at 4°C for 1 hr. The cells were then pulsed for 5 min at
552 37°C with prewarmed buffers at either **(A)** pH 5 or **(B)** the indicated pH and then the buffer
553 was replaced with complete medium containing NH₄Cl to prevent infection via the normal
554 endocytic route. After 12-18 hr at 37°C, RLUC (an indicator of infection via FFPM) and FLUC
555 (to standardize transfected cell numbers) were measured. The ratio of *Renilla* to firefly luciferase
556 (RLUC/FLUC) was then **(A)** normalized to RLUC/FLUC ratio for the mock-treated cells or **(B)**
557 directly plotted. Data are from a representative experiment performed with quintuplicate
558 samples. Error bars indicate SD. ***p < 0.001, **** p < 0.0001. Each experiment was repeated
559 one time with similar results.

560

561 **FIG 6. Arbidol impairs LASV GP1 dissociation from GP2.** **(A)** Flag-tagged LASV GP from
562 cell lysates of Lamp1 KO HEK293T/17 cells was immobilized on anti-Flag (M2) magnetic
563 beads, which were then treated with 0 or 40 μM arbidol for 1 hr at 4°C. The beads were then
564 subjected to a pulse for 1 min at 37°C at the indicated pH in the presence or absence of arbidol.
565 The extent of GP1 dissociation was then determined by Western blot analysis of GP1 in the
566 supernatant and bead-bound fractions. Data are the averages from four experiments. Error bars
567 represent SEM. **(B)** Flag-tagged LASV GP, prepared and immobilized as in panel **(A)**, was
568 pretreated with 0 or 40 μM arbidol. The beads were then exposed to pH 6.5, at 37°C for the

569 indicated time, in the presence or absence of arbidol, and the extent of GP1 dissociation
570 determined as in panel (A). Data are the averages from five experiments. Error bars represent
571 SEM.
572
573

574 REFERENCES

- 575 1. **Hallam HJ, Hallam S, Rodriguez SE, Barrett ADT, Beasley DWC, Chua A, Ksiazek**
576 **TG, Milligan GN, Sathiyamoorthy V, Reece LM.** 2018. Baseline mapping of Lassa
577 fever virology, epidemiology and vaccine research and development. *NPJ Vaccines* **3**:11.
- 578 2. **Siddle KJ, Eromon P, Barnes KG, Mehta S, Oguzie JU, Odia I, Schaffner SF,**
579 **Winnicki SM, Shah RR, Qu J, Wohl S, Brehio P, Iruolagbe C, Aiyepada J, Uyigue E,**
580 **Akhiolomen P, Okonofua G, Ye S, Kayode T, Ajogbasile F, Uwanibe J, Gaye A,**
581 **Momoh M, Chak B, Kotliar D, Carter A, Gladden-Young A, Freije CA, Omoregie O,**
582 **Osiemi B, Muoebonam EB, Airende M, Enigbe R, Ebo B, Nosamiefan I, Oluniyi P,**
583 **Nekoui M, Ogbaini-Emovon E, Garry RF, Andersen KG, Park DJ, Yozwiak NL,**
584 **Akpede G, Ihekweazu C, Tomori O, Okogbenin S, Folarin OA, Okokhere PO,**
585 **MacInnis BL, Sabeti PC, Happi CT.** 2018. Genomic Analysis of Lassa Virus during an
586 Increase in Cases in Nigeria in 2018. *N Engl J Med* **379**:1745–1753.
- 587 3. **Warner BM, Safronetz D, Stein DR.** 2018. Current research for a vaccine against Lassa
588 hemorrhagic fever virus. *Drug Des Devel Ther* **12**:2519–2527.
- 589 4. **Asogun DA, Adomeh DI, Ehimuan J, Odia I, Hass M, Gabriel M, Olschläger S,**
590 **Becker-Ziaja B, Folarin O, Phelan E, Ehiane PE, Ifeh VE, Uyigue EA, Oladapo YT,**
591 **Muoebonam EB, Osunde O, Dongo A, Okokhere PO, Okogbenin SA, Momoh M,**
592 **Alikah SO, Akhuemokhan OC, Imomeh P, Odike MAC, Gire S, Andersen K, Sabeti**
593 **PC, Happi CT, Akpede GO, Günther S.** 2012. Molecular diagnostics for lassa fever at
594 Irrua specialist teaching hospital, Nigeria: lessons learnt from two years of laboratory
595 operation. *PLoS Negl Trop Dis* **6**:e1839.
- 596 5. **Bausch DG, Hadi CM, Khan SH, Lertora J JL.** 2010. Review of the literature and
597 proposed guidelines for the use of oral ribavirin as postexposure prophylaxis for Lassa
598 fever. *Clin Infect Dis* **51**:1435–1441.
- 599 6. **Welch SR, Guerrero LW, Chakrabarti AK, McMullan LK, Flint M, Bluemling GR,**
600 **Painter GR, Nichol ST, Spiropoulou CF, Albariño CG.** 2016. Lassa and Ebola virus
601 inhibitors identified using minigenome and recombinant virus reporter systems. *Antiviral*
602 *Research* **136**:9–18.
- 603 7. **Goba A, Khan SH, Fonnies M, Fullah M, Moigboi A, Kovoma A, Sinnah V, Yoko N,**
604 **Rogers H, Safai S, Momoh M, Koroma V, Kamara FK, Konowu E, Yillah M, French**
605 **I, Mustapha I, Kanneh F, Foday M, McCarthy H, Kallon T, Kallon M, Naiebu J,**
606 **Sellu J, Jalloh AA, Gbakie M, Kanneh L, Massaly JLB, Kargbo D, Kargbo B, Vandi**
607 **M, Gbetuwa M, Gevao SM, Sandi JD, Jalloh SC, Grant DS, Blyden SO, Crozier I,**
608 **Schieffelin JS, McLellan SL, Jacob ST, Boisen ML, Hartnett JN, Cross RW, Branco**
609 **LM, Andersen KG, Yozwiak NL, Gire SK, Tariyal R, Park DJ, Haislip AM, Bishop**
610 **CM, Melnik LI, Gallaher WR, Wimley WC, He J, Shaffer JG, Sullivan BM, Grillo S,**
611 **Oman S, Garry CE, Edwards DR, McCormick SJ, Elliott DH, Rouelle JA,**
612 **Kannadka CB, Reyna AA, Bradley BT, Yu H, Yenni RE, Hastie KM, Geisbert JB,**
613 **Kulakosky PC, Wilson RB, Oldstone MBA, Pitts KR, Henderson LA, Robinson JE,**

- 614 **Geisbert TW, Saphire EO, Happi CT, Asogun DA, Sabeti PC, Garry RF, Viral**
615 **Hemorrhagic Fever Consortium.** 2016. An Outbreak of Ebola Virus Disease in the
616 Lassa Fever Zone. *J INFECT DIS* **214**:S110–S121.
- 617 8. **Wang P, Liu Y, Zhang G, Wang S, Guo J, Cao J, Jia X, Zhang L, Xiao G, Wang W.**
618 2018. Screening and Identification of Lassa Virus Entry Inhibitors from an FDA-
619 Approved Drug Library. *Journal of Virology* **92**:e00954–18.
- 620 9. **Ngo N, Henthorn KS, Cisneros MI, Cubitt B, Iwasaki M, la Torre de JC, Lama J.**
621 2015. Identification and Mechanism of Action of a Novel Small-Molecule Inhibitor of
622 Arenavirus Multiplication. *Journal of Virology* **89**:10924–10933.
- 623 10. **Rathbun JY, Droniou ME, Damoiseaux R, Haworth KG, Henley JE, Exline CM,**
624 **Choe H, Cannon PM.** 2015. Novel Arenavirus Entry Inhibitors Discovered by Using a
625 Minigenome Rescue System for High-Throughput Drug Screening. *Journal of Virology*
626 **89**:8428–8443.
- 627 11. **Shankar S, Whitby LR, Casquilho-Gray HE, York J, Boger DL, Nunberg JH.** 2016.
628 Small-Molecule Fusion Inhibitors Bind the pH-Sensing Stable Signal Peptide-GP2
629 Subunit Interface of the Lassa Virus Envelope Glycoprotein. *Journal of Virology*
630 **90**:6799–6807.
- 631 12. **Wang MK-M, Ren T, Liu H, Lim S-Y, Lee K, Honko A, Zhou H, Dyall J, Hensley L,**
632 **Gartin AK, Cunningham JM.** 2018. Critical role for cholesterol in Lassa fever virus
633 entry identified by a novel small molecule inhibitor targeting the viral receptor LAMP1.
634 *PLoS Pathog* **14**:e1007322.
- 635 13. **Burgeson JR, Moore AL, Gharaibeh DN, Larson RA, Cerruti NR, Amberg SM,**
636 **Hruby DE, Dai D.** 2013. Discovery and optimization of potent broad-spectrum arenavirus
637 inhibitors derived from benzimidazole and related heterocycles. *Bioorganic & Medicinal*
638 *Chemistry Letters* **23**:750–756.
- 639 14. **Rosenke K, Feldmann H, Westover JB, Hanley PW, Martellaro C, Feldmann F,**
640 **Saturday G, Lovaglio J, Scott DP, Furuta Y, Komeno T, Gowen BB, Safronetz D.**
641 2018. Use of Favipiravir to Treat Lassa Virus Infection in Macaques. *Emerging Infect Dis*
642 **24**:1696–1699.
- 643 15. **Urata S, Yun N, Pasquato A, Paessler S, Kunz S, la Torre de JC.** 2011. Antiviral
644 activity of a small-molecule inhibitor of arenavirus glycoprotein processing by the cellular
645 site 1 protease. *Journal of Virology* **85**:795–803.
- 646 16. **Mohr EL, McMullan LK, Lo MK, Spengler JR, Bergeron É, Albariño CG,**
647 **Shrivastava-Ranjan P, Chiang C-F, Nichol ST, Spiropoulou CF, Flint M.** 2015.
648 Inhibitors of cellular kinases with broad-spectrum antiviral activity for hemorrhagic fever
649 viruses. *Antiviral Research* **120**:40–47.
- 650 17. **Chou Y-Y, Cuevas C, Carocci M, Stubbs SH, Ma M, Cureton DK, Chao L, Evesson**
651 **F, He K, Yang PL, Whelan SP, Ross SR, Kirchhausen T, Gaudin R.** 2016.

- 652 Identification and Characterization of a Novel Broad-Spectrum Virus Entry Inhibitor.
653 *Journal of Virology* **90**:4494–4510.
- 654 18. **Gehring G, Rohrmann K, Atenchong N, Mittler E, Becker S, Dahlmann F,**
655 **Pöhlmann S, Vondran FWR, David S, Manns MP, Ciesek S, Hahn von T.** 2014. The
656 clinically approved drugs amiodarone, dronedarone and verapamil inhibit filovirus cell
657 entry. *Journal of Antimicrobial Chemotherapy* **69**:2123–2131.
- 658 19. **Johansen LM, Brannan JM, Delos SE, Shoemaker CJ, Stossel A, Lear C, Hoffstrom**
659 **BG, DeWald LE, Schornberg KL, Scully C, Lehar J, Hensley LE, White JM, Olinger**
660 **GG.** 2013. FDA-Approved Selective Estrogen Receptor Modulators Inhibit Ebola Virus
661 Infection. *Science Translational Medicine* **5**:190ra79–190ra79.
- 662 20. **Johansen LM, DeWald LE, Shoemaker CJ, Hoffstrom BG, Lear-Rooney CM, Stossel**
663 **A, Nelson E, Delos SE, Simmons JA, Grenier JM, Pierce LT, Pajouhesh H, Lehár J,**
664 **Hensley LE, Glass PJ, White JM, Olinger GG.** 2015. A screen of approved drugs and
665 molecular probes identifies therapeutics with anti-Ebola virus activity. *Science*
666 *Translational Medicine* **7**:290ra89–290ra89.
- 667 21. **Madrid PB, Chopra S, Manger ID, Gilfillan L, Keepers TR, Shurtleff AC, Green CE,**
668 **Iyer LV, Dilks HH, Davey RA, Kolokoltsov AA, Carrion R, Patterson JL, Bavari S,**
669 **Panchal RG, Warren TK, Wells JB, Moos WH, Burke RL, Tanga MJ.** 2013. A
670 Systematic Screen of FDA-Approved Drugs for Inhibitors of Biological Threat Agents.
671 *PLoS ONE* **8**:e60579–14.
- 672 22. **Kouznetsova J, Sun W, Martínez-Romero C, Tawa G, Shinn P, Chen CZ, Schimmer**
673 **A, Sanderson P, McKew JC, Zheng W, García-Sastre A.** 2014. Identification of 53
674 compounds that block Ebola virus-like particle entry via a repurposing screen of approved
675 drugs. *Emerg Microbes Infect* **3**:e84–e84.
- 676 23. **Dyall J, Nelson EA, DeWald LE, Guha R, Hart BJ, Zhou H, Postnikova E, Logue J,**
677 **Vargas WM, Gross R, Michelotti J, Deuliis N, Bennett RS, Crozier I, Holbrook MR,**
678 **Morris PJ, Klumpp-Thomas C, McKnight C, Mierzwa T, Shinn P, Glass PJ,**
679 **Johansen LM, Jahrling PB, Hensley LE, Olinger GG, Thomas C, White JM.** 2018.
680 Identification of Combinations of Approved Drugs With Synergistic Activity Against
681 Ebola Virus in Cell Cultures. *J INFECT DIS* **9**:299.
- 682 24. **Rhein BA, Maury WJ.** 2015. Ebola virus entry into host cells: identifying therapeutic
683 strategies. *Curr Clin Microbiol Rep* **2**:115–124.
- 684 25. **Jae LT, Brummelkamp TR.** 2015. Emerging intracellular receptors for hemorrhagic
685 fever viruses. *Trends in Microbiology* **23**:1–9.
- 686 26. **Jae LT, Raaben M, Herbert AS, Kuehne AI, Wirchnianski AS, Soh TK, Stubbs SH,**
687 **Janssen H, Damme M, Saftig P, Whelan SP, Dye JM, Brummelkamp TR.** 2014. Lassa
688 virus entry requires a trigger-induced receptor switch. *Science* **344**:1506–1510.

- 689 27. **Carette JE, Raaben M, Wong AC, Herbert AS, Obernosterer G, Mulherkar N,**
690 **Kuehne AI, Kranzusch PJ, Griffin AM, Ruthel G, Cin PD, Dye JM, Whelan SP,**
691 **Chandran K, Brummelkamp TR.** 2011. Ebola virus entry requires the cholesterol
692 transporter Niemann-Pick C1. *Nature* **477**:340–343.
- 693 28. **Côté M, Misasi J, Ren T, Bruchez A, Lee K, Filone CM, Hensley L, Li Q, Ory D,**
694 **Chandran K, Cunningham J.** 2011. Small molecule inhibitors reveal Niemann-Pick C1
695 is essential for Ebola virus infection. *Nature* **477**:344–348.
- 696 29. **Brouillette RB, Phillips EK, Patel R, Mahauad-Fernandez W, Moller-Tank S, Rogers**
697 **KJ, Dillard JA, Cooney AL, Martinez-Sobrido L, Okeoma C, Maury W.** 2018. TIM-1
698 Mediates Dystroglycan-Independent Entry of Lassa Virus. *Journal of Virology*
699 **92**:e00093–18.
- 700 30. **Oppliger J, Torriani G, Herrador A, Kunz S.** 2016. Lassa Virus Cell Entry via
701 Dystroglycan Involves an Unusual Pathway of Macropinocytosis. *Journal of Virology*
702 **90**:6412–6429.
- 703 31. **Hulseberg CE, Fénéant L, Szymańska KM, White JM.** 2018. Lamp1 Increases the
704 Efficiency of Lassa Virus Infection by Promoting Fusion in Less Acidic Endosomal
705 Compartments. *mBio* **9**:e01818–17.
- 706 32. **Fedeli C, Moreno H, Kunz S.** 2018. Novel Insights into Cell Entry of Emerging Human
707 Pathogenic Arenaviruses. *J Mol Biol* **430**:1839–1852.
- 708 33. **Fink SL, Vojtech L, Wagoner J, Slivinski NSJ, Jackson KJ, Wang R, Khadka S,**
709 **Luthra P, Basler CF, Polyak SJ.** 2018. The Antiviral Drug Arbidol Inhibits Zika Virus.
710 *Sci Rep* **8**:8989.
- 711 34. **Pécheur E-I, Borisevich V, Halfmann P, Morrey JD, Smee DF, Prichard M, Mire CE,**
712 **Kawaoka Y, Geisbert TW, Polyak SJ.** 2016. The Synthetic Antiviral Drug Arbidol
713 Inhibits Globally Prevalent Pathogenic Viruses. *Journal of Virology* **90**:3086–3092.
- 714 35. **Teissier E, Zandomenighi G, Loquet A, Lavillette D, Lavergne J-P, Montserret R,**
715 **Cosset F-L, Böckmann A, Meier BH, Penin F, Pécheur E-I.** 2011. Mechanism of
716 inhibition of enveloped virus membrane fusion by the antiviral drug arbidol. *PLoS ONE*
717 **6**:e15874.
- 718 36. **Blaising J, Polyak SJ, Pécheur E-I.** 2014. Arbidol as a broad-spectrum antiviral: an
719 update. *Antiviral Research* **107**:84–94.
- 720 37. **Leneva IA, Russell RJ, Boriskin YS, Hay AJ.** 2009. Characteristics of arbidol-resistant
721 mutants of influenza virus: implications for the mechanism of anti-influenza action of
722 arbidol. *Antiviral Research* **81**:132–140.
- 723 38. **Kadam RU, Wilson IA.** 2017. Structural basis of influenza virus fusion inhibition by the
724 antiviral drug Arbidol. *Proc Natl Acad Sci USA* **114**:206–214.

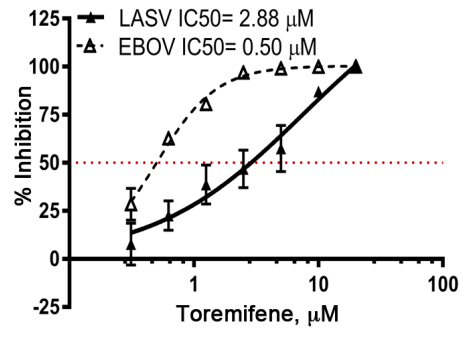
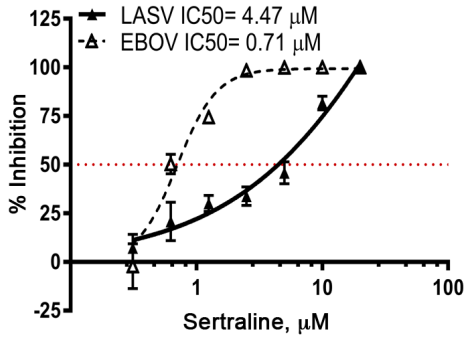
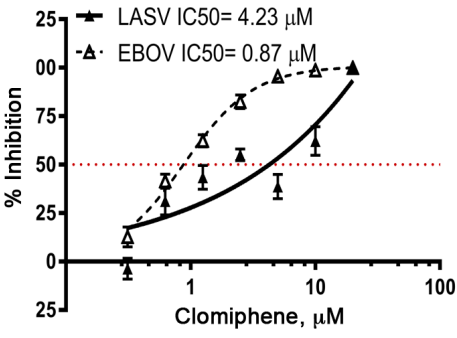
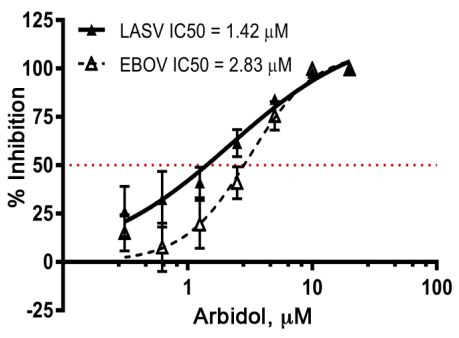
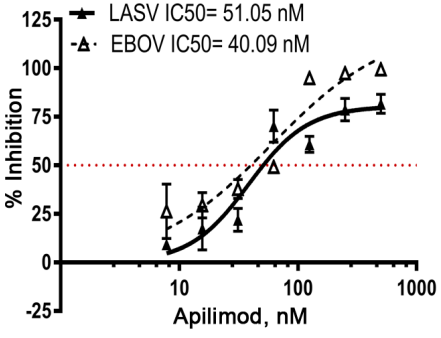
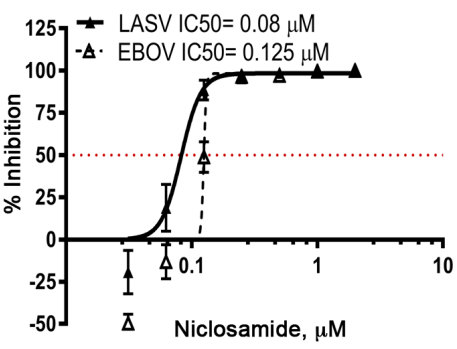
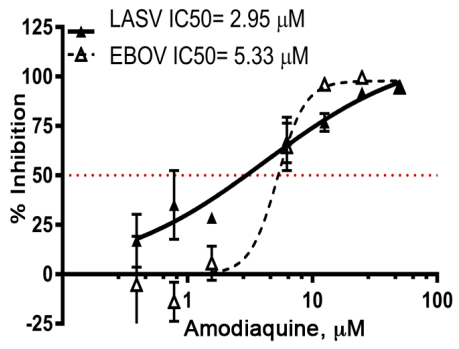
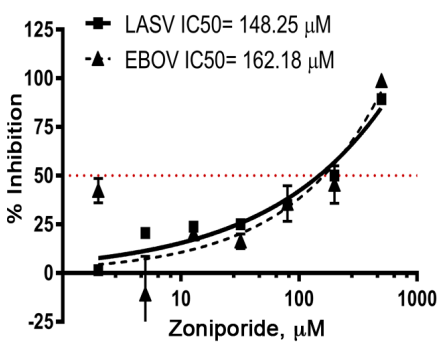
- 725 39. **Brancato V, Peduto A, Wharton S, Martin S, More V, Di Mola A, Massa A, Perfetto**
726 **B, Donnarumma G, Schiraldi C, Tufano MA, de Rosa M, Filosa R, Hay A.** 2013.
727 Design of inhibitors of influenza virus membrane fusion: synthesis, structure-activity
728 relationship and in vitro antiviral activity of a novel indole series. *Antiviral Research*
729 **99**:125–135.
- 730 40. **Shoemaker CJ, Schornberg KL, Delos SE, Scully C, Pajouhesh H, Olinger GG,**
731 **Johansen LM, White JM.** 2013. Multiple Cationic Amphiphiles Induce a Niemann-Pick
732 C Phenotype and Inhibit Ebola Virus Entry and Infection. *PLoS ONE* **8**:e56265–13.
- 733 41. **Boriskin YS, Pécheur E-I, Polyak SJ.** 2006. Arbidol: a broad-spectrum antiviral that
734 inhibits acute and chronic HCV infection. *Virol J* **3**:56.
- 735 42. **Cohen-Dvashi H, Israeli H, Shani O, Katz A, Diskin R.** 2016. Role of LAMP1 Binding
736 and pH Sensing by the Spike Complex of Lassa Virus. *Journal of Virology* **90**:10329–
737 10338.
- 738 43. **Kondo N, Miyauchi K, Matsuda Z.** 2011. Monitoring viral-mediated membrane fusion
739 using fluorescent reporter methods. *Curr Protoc Cell Biol* **Chapter 26**:Unit 26.9–26.9.9.
- 740 44. **Wright ZVF, Wu NC, Kadam RU, Wilson IA, Wolan DW.** 2017. Structure-based
741 optimization and synthesis of antiviral drug Arbidol analogues with significantly
742 improved affinity to influenza hemagglutinin. *Bioorganic & Medicinal Chemistry Letters*
743 **27**:3744–3748.
- 744 45. **Boriskin YS, Leneva IA, Pecheur EI, Polyak SP.** 2008. Arbidol: A Broad-Spectrum
745 Antiviral Compound that Blocks Viral Fusion. *Current Medicinal Chemistry* **15**:997–1005.
- 746 46. **Illick MM, Branco LM, Fair JN, Illick KA, Matschiner A, Schoepp R, Garry RF,**
747 **Guttieri MC.** 2008. Uncoupling GP1 and GP2 expression in the Lassa virus glycoprotein
748 complex: implications for GP1 ectodomain shedding. *Virol J* **5**:161.
- 749 47. **Klewitz C, Klenk H-D, Meulen ter J.** 2007. Amino acids from both N-terminal
750 hydrophobic regions of the Lassa virus envelope glycoprotein GP-2 are critical for pH-
751 dependent membrane fusion and infectivity. *Journal of General Virology* **88**:2320–2328.
- 752 48. **Li S, Sun Z, Pryce R, Parsy M-L, Fehling SK, Schlie K, Siebert CA, Garten W,**
753 **Bowden TA, Strecker T, Huiskonen JT.** 2016. Acidic pH-Induced Conformations and
754 LAMP1 Binding of the Lassa Virus Glycoprotein Spike. *PLoS Pathog* **12**:e1005418–18.
- 755 49. **White JM, Whittaker GR.** 2016. Fusion of Enveloped Viruses in Endosomes. *Traffic*
756 **17**:593–614.
- 757 50. **Madrid PB, Panchal RG, Warren TK, Shurtleff AC, Endsley AN, Green CE,**
758 **Kolokoltsov A, Davey R, Manger ID, Gilfillan L, Bavari S, Tanga MJ.** 2015.
759 Evaluation of Ebola Virus Inhibitors for Drug Repurposing. *ACS Infect Dis* **1**:317–326.

- 760 51. **Nelson EA, Dyall J, Hoenen T, Barnes AB, Zhou H, Liang JY, Michelotti J, Dewey**
761 **WH, DeWald LE, Bennett RS, Morris PJ, Guha R, Klumpp-Thomas C, McKnight C,**
762 **Chen Y-C, Xu X, Wang A, Hughes E, Martin S, Thomas C, Jahrling PB, Hensley LE,**
763 **Olinger GG, White JM.** 2017. The phosphatidylinositol-3-phosphate 5-kinase inhibitor
764 apilimod blocks filoviral entry and infection. *PLoS Negl Trop Dis* **11**:e0005540.
- 765 52. **Iwasaki M, Ngo N, la Torre de JC.** 2013. Sodium Hydrogen Exchangers Contribute to
766 Arenavirus Cell Entry. *Journal of Virology* **88**:643–654.
- 767 53. **Qiu S, Leung A, Bo Y, Kozak RA, Anand SP, Warkentin C, Salambanga FDR, Cui J,**
768 **Kobinger G, Kobasa D, Côté M.** 2018. Ebola virus requires phosphatidylinositol (3,5)
769 bisphosphate production for efficient viral entry. *Virology* **513**:17–28.
- 770 54. **Vigant F, Santos NC, Lee B.** 2015. Broad-spectrum antivirals against viral fusion. *Nature*
771 *Reviews Microbiology* **13**:426–437.
- 772 55. **Saeed MF, Kolokoltsov AA, Albrecht T, Davey RA.** 2010. Cellular Entry of Ebola
773 Virus Involves Uptake by a Macropinocytosis-Like Mechanism and Subsequent
774 Trafficking through Early and Late Endosomes. *PLoS Pathog* **6**:e1001110–15.
- 775 56. **Nanbo A, Imai M, Watanabe S, Noda T, Takahashi K, Neumann G, Halfmann P,**
776 **Kawaoka Y.** 2010. Ebola virus Is Internalized into Host Cells via Macropinocytosis in a
777 Viral Glycoprotein-Dependent Manner. *PLoS Pathog* **6**:e1001121–20.
- 778 57. **Jurgeit A, McDowell R, Moese S, Meldrum E, Schwendener R, Greber UF.** 2012.
779 Niclosamide Is a Proton Carrier and Targets Acidic Endosomes with Broad Antiviral
780 Effects. *PLoS Pathog* **8**:e1002976–14.
- 781 58. **Zilbermintz L, Leonardi W, Jeong S-Y, Sjodt M, McComb R, Ho C-LC, Retterer C,**
782 **Gharaibeh D, Zamani R, Soloveva V, Bavari S, Levitin A, West J, Bradley KA,**
783 **Clubb RT, Cohen SN, Gupta V, Martchenko M.** 2015. Identification of agents effective
784 against multiple toxins and viruses by host-oriented cell targeting. *Sci Rep* **5**:13476.
- 785 59. **Sakurai Y, Sakakibara N, Toyama M, Baba M, Davey RA.** 2018. Novel amodiaquine
786 derivatives potently inhibit Ebola virus infection. *Antiviral Research* **160**:175–182.
- 787 60. **Marois I, Cloutier A, Meunier I, Weingartl HM, Cantin AM, Richter MV.** 2014.
788 Inhibition of influenza virus replication by targeting broad host cell pathways. *PLoS ONE*
789 **9**:e110631.
- 790 61. **Cai X, Xu Y, Cheung AK, Tomlinson RC, Alcázar-Román A, Murphy L, Billich A,**
791 **Zhang B, Feng Y, Klumpp M, Rondeau J-M, Fazal AN, Wilson CJ, Myer V, Joberty**
792 **G, Bouwmeester T, Labow MA, Finan PM, Porter JA, Ploegh HL, Baird D, Pietro**
793 **De Camilli, Tallarico JA, Huang Q.** 2013. PIKfyve, a Class III PI Kinase, Is the Target
794 of the Small Molecular IL-12/IL-23 Inhibitor Apilimod and a Player in Toll-like Receptor
795 Signaling. *Chemistry & Biology* **20**:912–921.

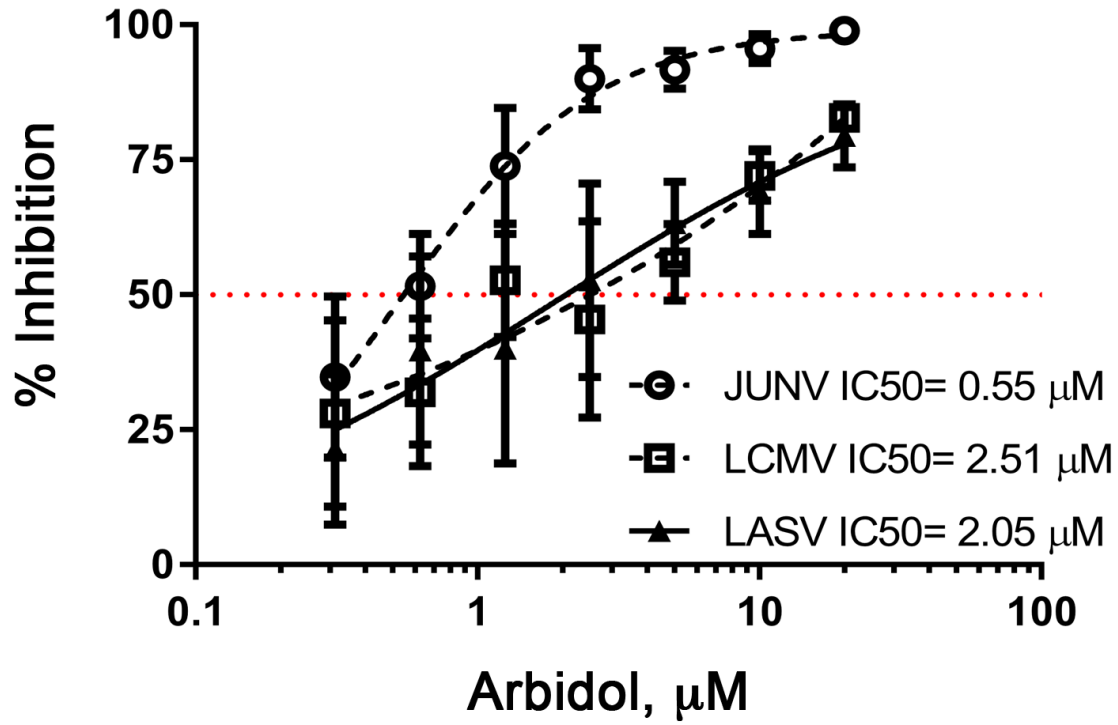
- 796 62. **Mingo RM, Simmons JA, Shoemaker CJ, Nelson EA, Schornberg KL, D'Souza RS,**
797 **Casanova JE, White JM.** 2015. Ebola Virus and Severe Acute Respiratory Syndrome
798 Coronavirus Display Late Cell Entry Kinetics: Evidence that Transport to NPC1
799 +Endolysosomes Is a Rate-Defining Step. *Journal of Virology* **89**:2931–2943.
- 800 63. **Simmons JA, D'Souza RS, Ruas M, Galione A, Casanova JE, White JM.** 2016.
801 Ebolavirus Glycoprotein Directs Fusion through NPC1+ Endolysosomes. *Journal of*
802 *Virology* **90**:605–610.
- 803 64. **Spence JS, Krause TB, Mittler E, Jangra RK, Chandran K.** 2016. Direct Visualization
804 of Ebola Virus Fusion Triggering in the Endocytic Pathway. *mBio* **7**:e01857–15–12.
- 805 65. **Miller EH, Obernosterer G, Raaben M, Herbert AS, Deffieu MS, Krishnan A,**
806 **Ndungo E, Sandesara RG, Carette JE, Kuehne AI, Ruthel G, Pfeffer SR, Dye JM,**
807 **Whelan SP, Brummelkamp TR, Chandran K.** 2016. Ebola virus entry requires the
808 host-programmed recognition of an intracellular receptor. *The EMBO Journal* **31**:1–14.
- 809 66. **Pécheur E-I, Lavillette D, Alcaras F, Molle J, Boriskin YS, Roberts M, Cosset F-L,**
810 **Polyak SJ.** 2007. Biochemical mechanism of hepatitis C virus inhibition by the broad-
811 spectrum antiviral arbidol. *Biochemistry* **46**:6050–6059.
- 812 67. **Gerlach T, Hensen L, Matrosovich T, Bergmann J, Winkler M, Peteranderl C,**
813 **Klenk H-D, Weber F, Herold S, Pöhlmann S, Matrosovich M.** 2017. pH Optimum of
814 Hemagglutinin-Mediated Membrane Fusion Determines Sensitivity of Influenza A
815 Viruses to the Interferon-Induced Antiviral State and IFITMs. *Journal of Virology*
816 **91**:e00246–17.
- 817 68. **Andrews P, Thyssen J, Lorke D.** 1982. The biology and toxicology of molluscicides,
818 Bayluscide (p282) **19**:245–295.
- 819 69. **Bixler SL, Duplantier AJ, Bavari S.** 2017. Discovering Drugs for the Treatment of
820 Ebola Virus. *Curr Treat Options Infect Dis* **9**:299–317.
- 821 70. **Krausz S, Boumans MJH, Gerlag DM, Lufkin J, van Kuijk AWR, Bakker A, de**
822 **Boer M, Lodde BM, Reedquist KA, Jacobson EW, O'Meara M, Tak PP.** 2012. Brief
823 report: a phase IIa, randomized, double-blind, placebo-controlled trial of apilimod
824 mesylate, an interleukin-12/interleukin-23 inhibitor, in patients with rheumatoid arthritis.
825 *Arthritis Rheum* **64**:1750–1755.
- 826 71. **Haviernik J, Štefánik M, Fojtíková M, Kali S, Tordo N, Rudolf I, Hubálek Z, Eyer L,**
827 **Ruzek D.** 2018. Arbidol (Umifenovir): A Broad-Spectrum Antiviral Drug That Inhibits
828 Medically Important Arthropod-Borne Flaviviruses. *Viruses* **10**:184.
- 829 72. **Deng P, Zhong D, Yu K, Zhang Y, Wang T, Chen X.** 2013. Pharmacokinetics,
830 metabolism, and excretion of the antiviral drug arbidol in humans. *Antimicrobial Agents*
831 *and Chemotherapy* **57**:1743–1755.

- 832 73. **Liu MY, et A.** Pharmacokinetic properties and bioequivalence of two formulations of
833 arbidol: an open-label, single-dose, randomized-sequence, two-period crossover study in
834 healthy Chinese male volunteers. *Clinical therapeutics* **31**:784–792.
- 835 74. **Sun Y, et A.** 2013. Pharmacokinetics of single and multiple oral doses of arbidol in
836 healthy Chinese volunteers. *International Journal of clinical pharmacology and*
837 *therapeutics* **51**:423–432.
- 838 75. **Leneva IA, Burtseva EI, Yatsyshina SB, Fedyakina IT, Kirillova ES, Selkova EP,**
839 **Osipova E, Maleev VV.** 2016. Virus susceptibility and clinical effectiveness of anti-
840 influenza drugs during the 2010-2011 influenza season in Russia. *Int J Infect Dis* **43**:77–
841 84.
- 842 76. **Oestereich L, Rieger T, Neumann M, Bernreuther C, Lehmann M, Krasemann S,**
843 **Wurr S, Emmerich P, de Lamballerie X, Olschläger S, Günther S.** 2014. Evaluation
844 of antiviral efficacy of ribavirin, arbidol, and T-705 (favipiravir) in a mouse model for
845 Crimean-Congo hemorrhagic fever. *PLoS Negl Trop Dis* **8**:e2804.
- 846 77. **Oestereich L, Rieger T, Lüdtke A, Ruibal P, Wurr S, Pallasch E, Bockholt S,**
847 **Krasemann S, Muñoz-Fontela C, Günther S.** 2016. Efficacy of Favipiravir Alone and
848 in Combination With Ribavirin in a Lethal, Immunocompetent Mouse Model of Lassa
849 Fever. *J INFECT DIS* **213**:934–938.
- 850 78. **Westover JB, Sefing EJ, Bailey KW, Van Wettere AJ, Jung K-H, Dagley A,**
851 **Wandersee L, Downs B, Smee DF, Furuta Y, Bray M, Gowen BB.** 2016. Low-dose
852 ribavirin potentiates the antiviral activity of favipiravir against hemorrhagic fever viruses.
853 *Antiviral Research* **126**:62–68.
- 854 79. **Leneva IA, Fedyakina IT, Guskova TA, Glushkov RG.** 2005. The sensitivity of various
855 influenza virus strains to arbidol. The influence of arbidol in combination with other
856 antiviral drugs on reproduction of influenza virus A. *Ther Arch Russian* **77**:84.
- 857 80. **Dyall J, Coleman CM, Hart BJ, Venkataraman T, Holbrook MR, Kindrachuk J,**
858 **Johnson RF, Olinger GG, Jahrling PB, Laidlaw M, Johansen LM, Lear-Rooney CM,**
859 **Glass PJ, Hensley LE, Frieman MB.** 2014. Repurposing of clinically developed drugs
860 for treatment of Middle East respiratory syndrome coronavirus infection. *Antimicrobial*
861 *Agents and Chemotherapy* **58**:4885–4893.
- 862 81. **Xu M, Lee EM, Wen Z, Cheng Y, Huang W-K, Qian X, Tew J, Kouznetsova J,**
863 **Ogden SC, Hammack C, Jacob F, Nguyen HN, Itkin M, Hanna C, Shinn P, Allen C,**
864 **Michael SG, Simeonov A, Huang W, Christian KM, Goate A, Brennand KJ, Huang**
865 **R, Xia M, Ming G-L, Zheng W, Song H, Tang H.** 2016. Identification of small-
866 molecule inhibitors of Zika virus infection and induced neural cell death via a drug
867 repurposing screen. *Nat Med* **22**:1101–1107.
- 868 82. **Kao J-C, HuangFu W-C, Tsai T-T, Ho M-R, Jhan M-K, Shen T-J, Tseng P-C, Wang**
869 **Y-T, Lin C-F.** 2018. The antiparasitic drug niclosamide inhibits dengue virus infection by

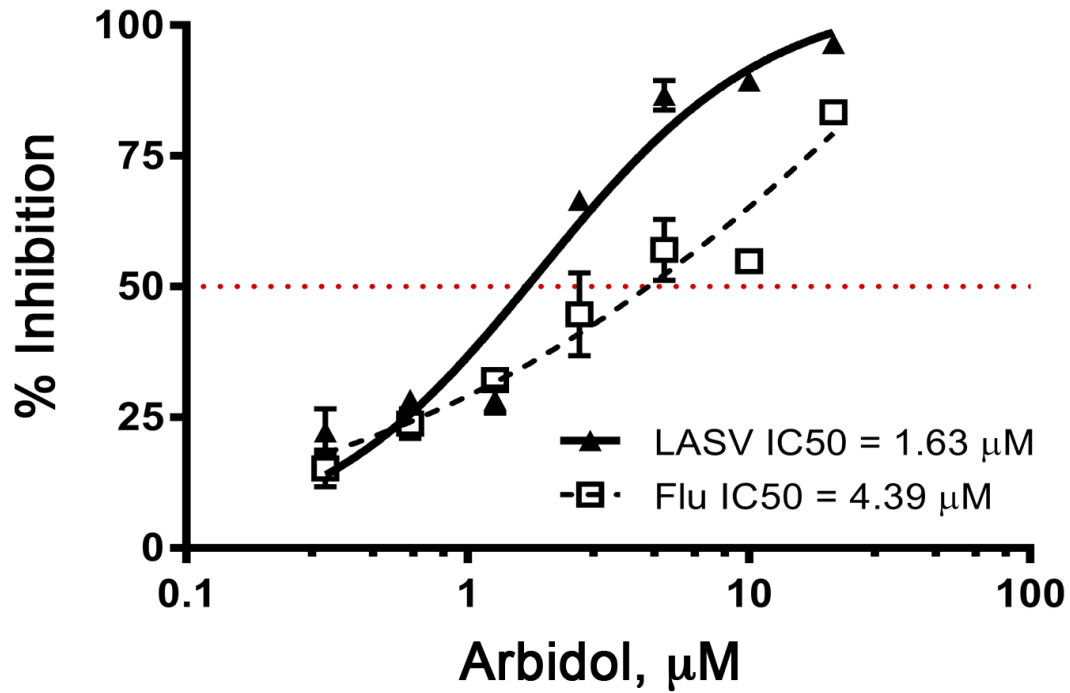
- 870 interfering with endosomal acidification independent of mTOR. PLoS Negl Trop Dis
871 **12:e0006715.**
- 872 83. **Wang Y-M, Lu J-W, Lin C-C, Chin Y-F, Wu T-Y, Lin L-I, Lai Z-Z, Kuo S-C, Ho Y-**
873 **J.** 2016. Antiviral activities of niclosamide and nitazoxanide against chikungunya virus
874 entry and transmission. Antiviral Research **135**:81–90.
- 875
- 876
- 877

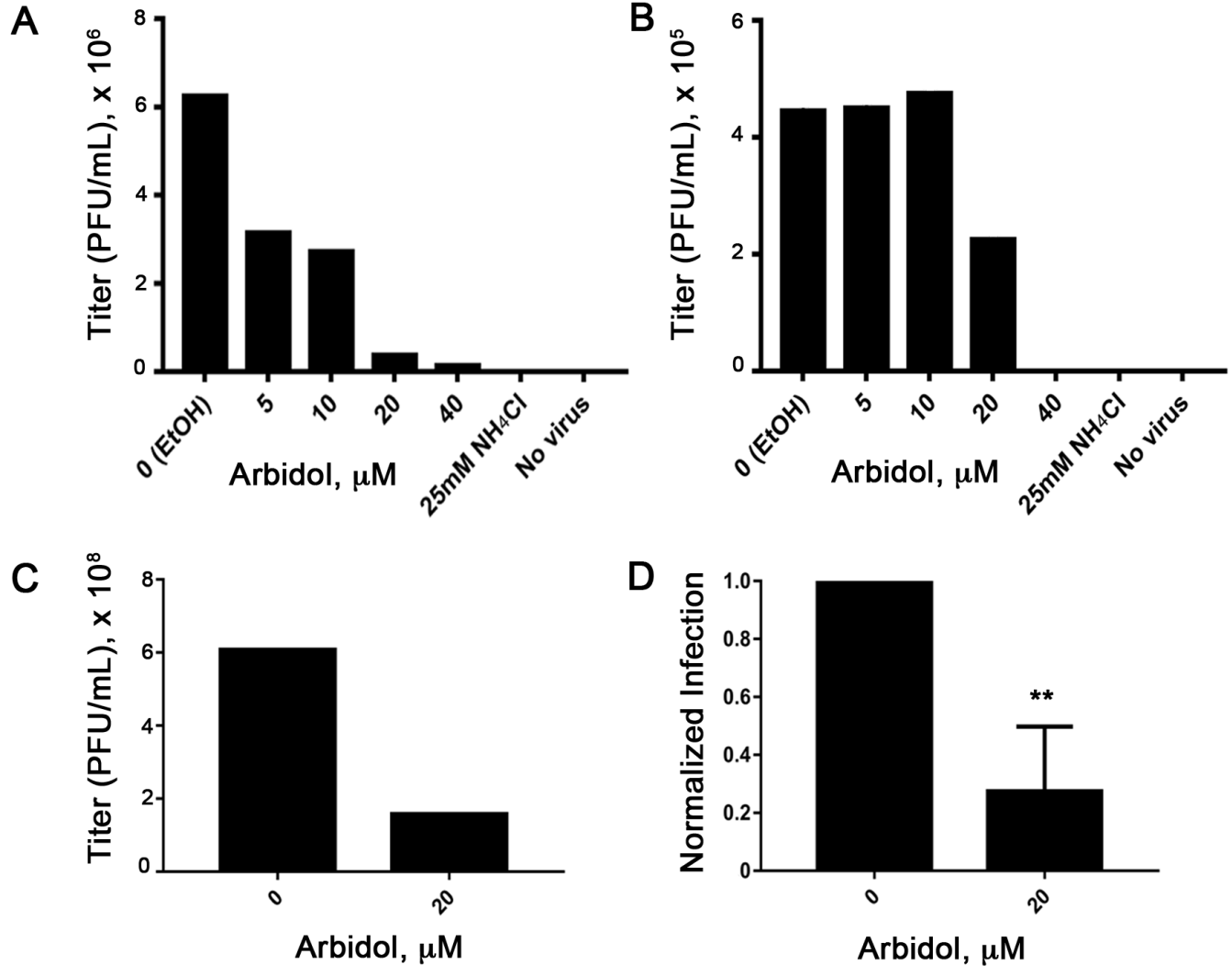


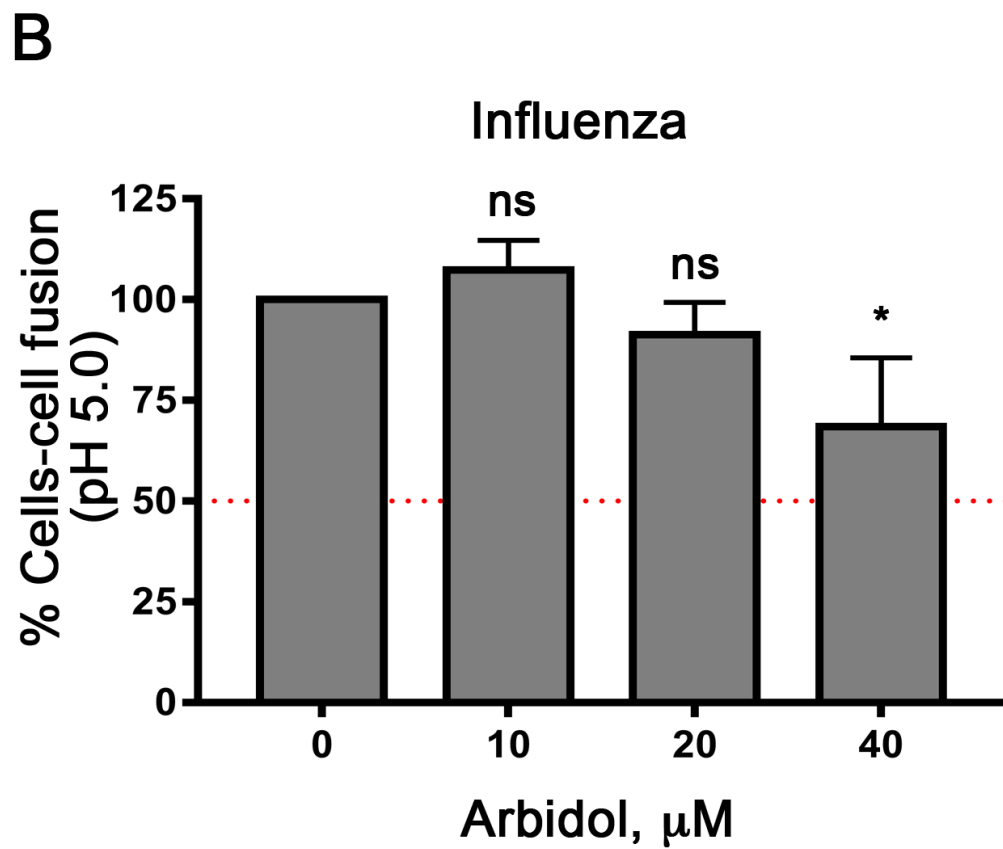
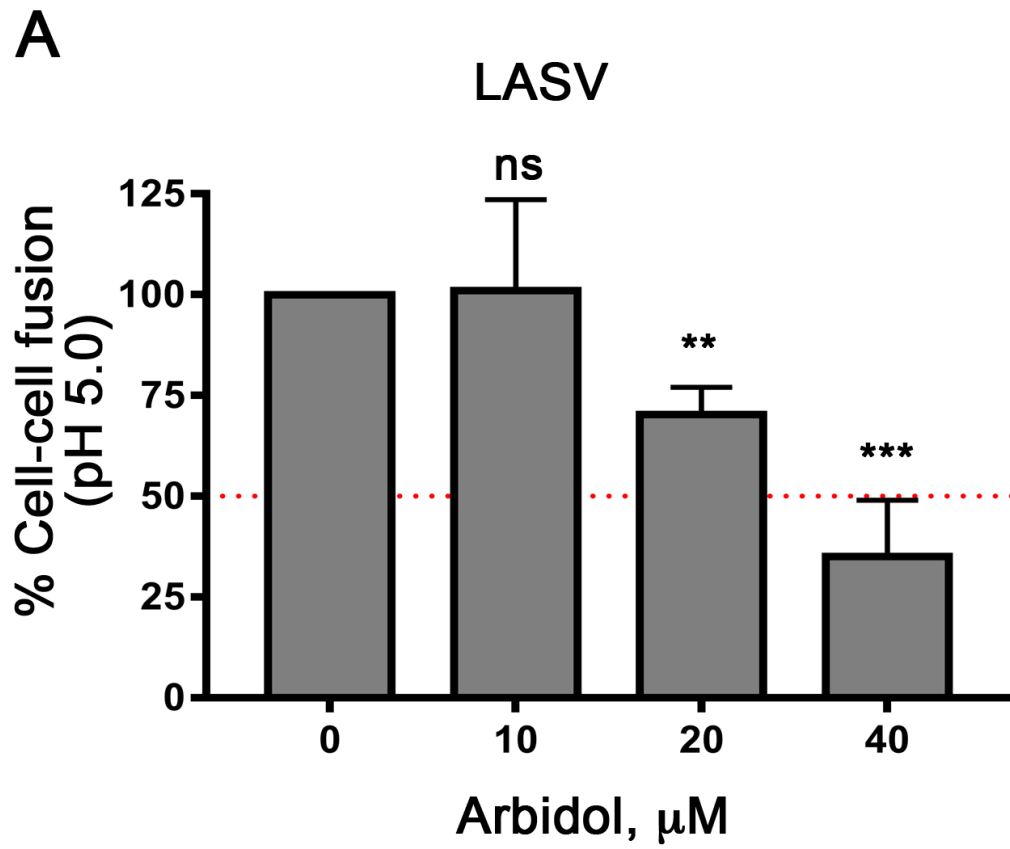
A

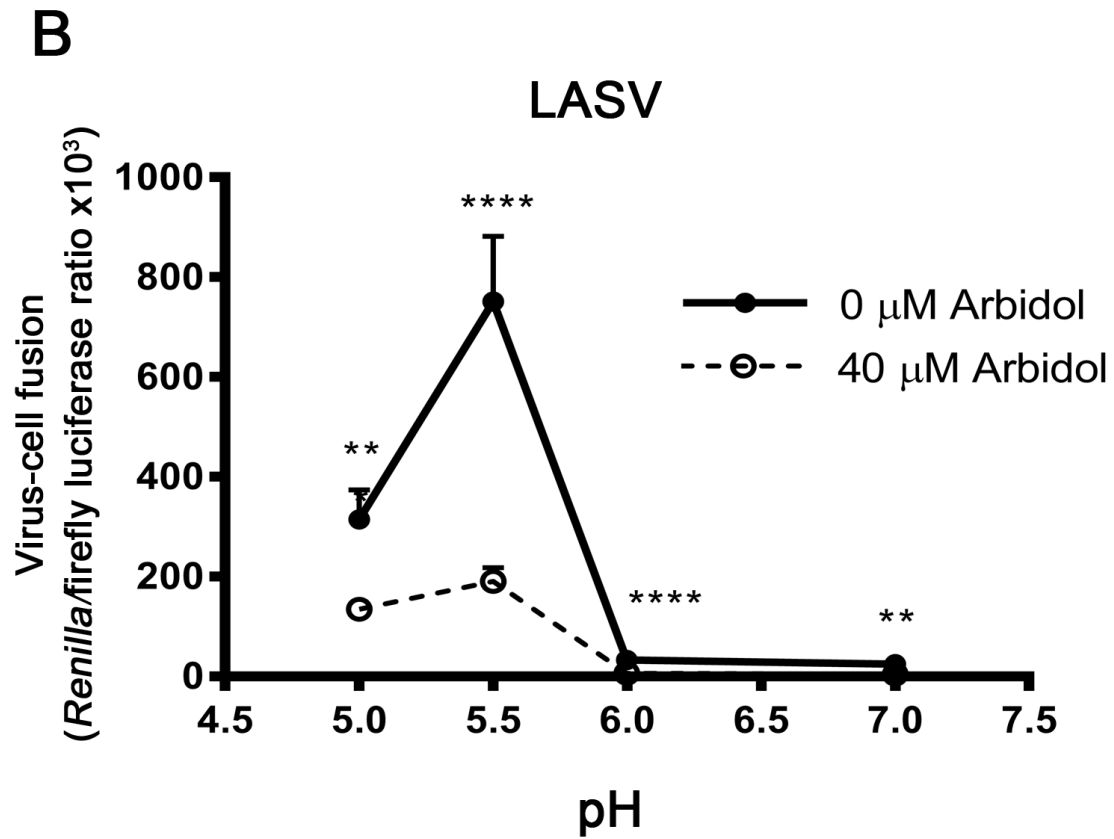
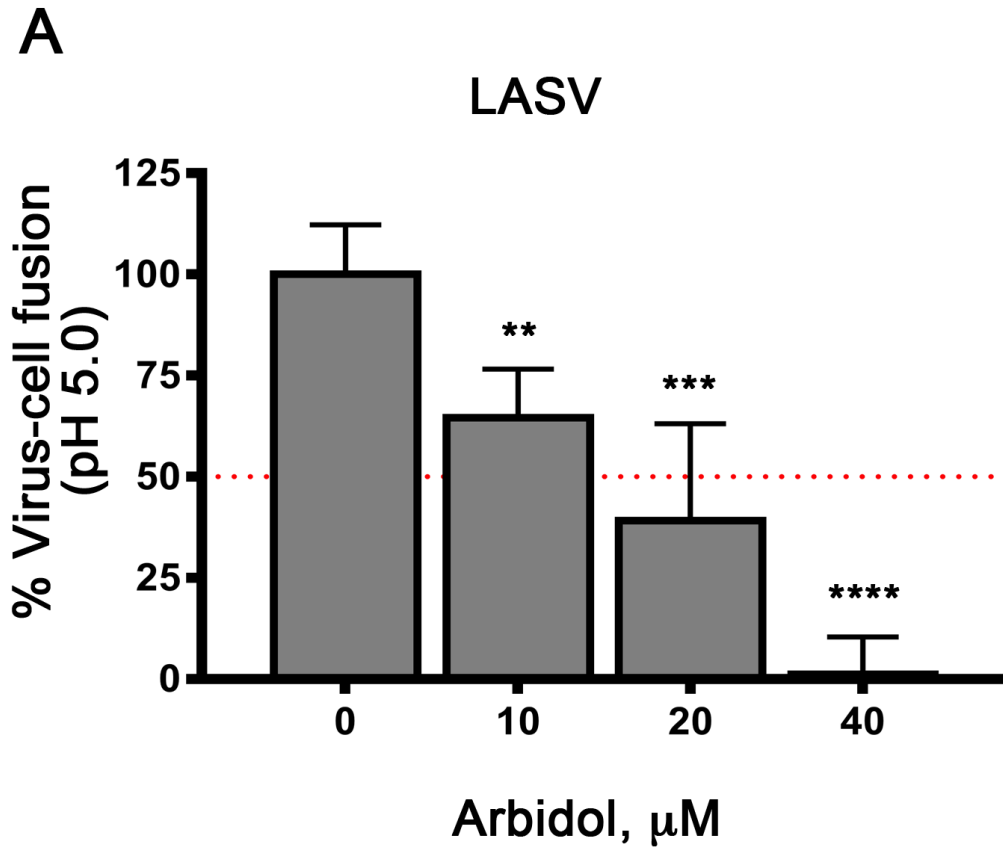


B

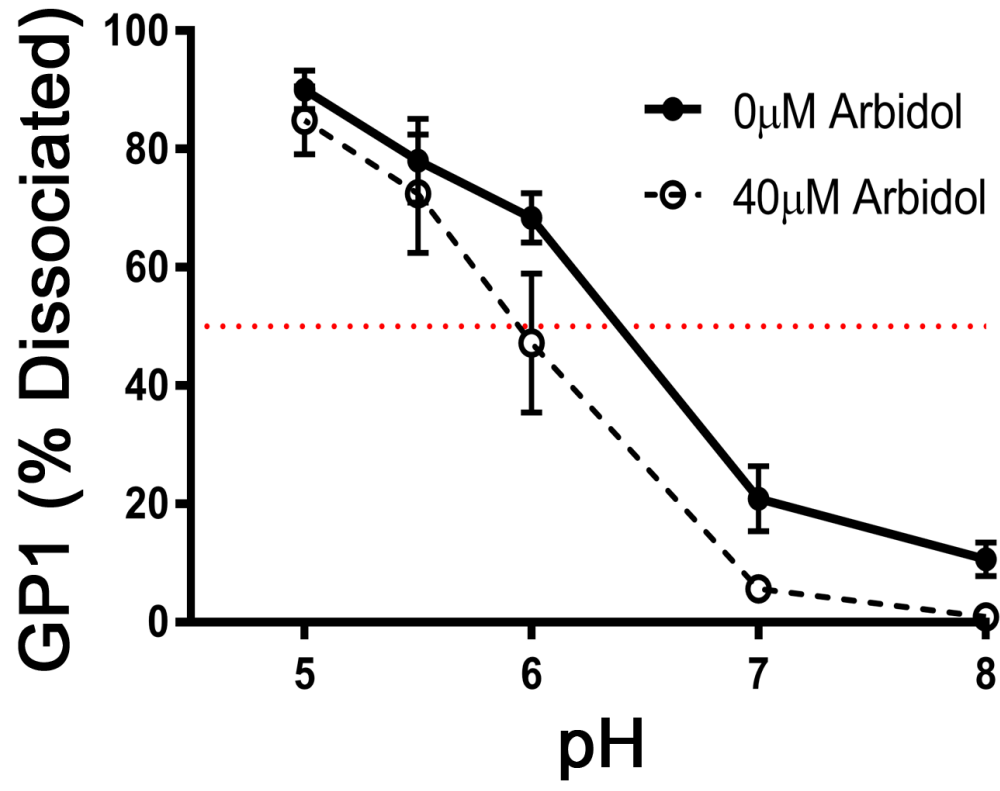








A



B

